Geological controls on the geometry of incised-valley fills: Insights from a global dataset of late-Quaternary examples

Ru Wang[1], Luca Colombera[1], and Nigel P. Mountney[1]

[1] Fluvial & Eolian Research Group, School of Earth & Environment, University of Leeds, Leeds, LS2 9JT, UK

ABSTRACT

Incised valleys that develop due to relative sea-level change are common features of continental shelves and coastal plains. Assessment of the factors that control the geometry of incised-valley fills has hitherto largely relied on conceptual, experimental or numerical models, else has been grounded on case studies of individual depositional systems. Here, a database-driven statistical analysis of 151 late-Quaternary incised-valley fills has been performed, the aim being to investigate the geological controls on their geometry.

Results of this analysis have been interpreted with consideration of the role of different processes in determining the geometry of incised-valley fills through their effect on the degree and rate of river incision, and on river size and mobility. The studied incised-valley fills developed along active margins are thicker and wider, on average, than those along passive margins, suggesting that tectonic setting exerts a control on the geometry of incised-valley fills, likely through effects on relative sea-level change and river behaviour, and in relation to distinct characteristics of basin physiography, water discharge and modes of sediment delivery. Valley-fill geometry is positively correlated with the associated drainage-basin size, confirming the dominant role of water discharge. Climate is also inferred to exert a potential control on valley-fill dimensions, possibly through modulations of temperature, peak precipitation, vegetation and permafrost, which would in turn affect water discharge, rates of sediment supply and valley-margin stability. Shelves with slope breaks that are currently deeper than 120 m contain incised-valley fills that are thicker and wider, on average, than those hosted on shelves with breaks shallower than 120 m. No correlation exists between valley-fill thickness and present-day coastal-prism convexity, which is measured as the difference in gradient between lower coastal plains and inner shelves.

These findings challenge some concepts embedded in sequence stratigraphic thinking, and have significant implications for analysis and improved understanding of source-to-sink sediment route-ways, and for attempting predictions of the occurrence and characteristics of hydrocarbon reservoirs.

Keywords: incised valley, sea-level change, drainage basin, basin physiography, Last Glacial Maximum, fluvial equilibrium profile.

INTRODUCTION

Incised valleys are common features of continental shelves and coastal plains. In these settings, valleys develop as fluvially eroded, elongated palaeotopographic lows in response to relative sea-level fall that causes rivers to incise their bed in an attempt to reach a new lowered equilibrium profile (Summerfield, 1985; Posamentier and Allen, 1999; Blum and Törnqvist, 2000; Holbrook et al., 2006; Blum et al., 2013). The resultant valleys are subsequently inundated by the sea during a following

episode of sea-level rise, typically leading to the development of estuaries in the nearshore (Zaitlin et al., 1994). As transgression proceeds, both the valley margins and the sedimentary infill in the base of the valley itself may be reworked by coastal and marine processes (Roy, 1984; Dalrymple et al., 1992; Allen and Posamentier, 1993; Zaitlin et al., 1994; Strong and Paola, 2008; Blum and Törnqvist, 2000; Blum et al., 2013). Valley systems that are cut in response to relative sea-level change possess greater potential for sediment accommodation than time-equivalent interfluve areas, and the infill of such valleys typically records a complex history of infilling via sedimentation in a range of environments as sea level rises (Thomas and Anderson, 1994; Rodriguez et al., 2005; Simms et al., 2007a).

Although incision and development of valleys in the nearshore region occurs during episodes of relative sea-level fall, valley development may continue during lowstand times as rivers seek to re-equilibrate (Summerfield, 1985; Blum and Price, 1998; Posamentier and Allen, 1999; Blum and Törnqvist, 2000; Holbrook et al., 2006; Strong and Paola, 2008; Martin et al., 2011; Blum et al., 2013). The lower part of the valley fill usually records sediment accumulation via fluvial systems both during the falling-stage and lowstand systems tracts (Blum and Price, 1998; Strong and Paola, 2008; Martin et al., 2011; Blum et al., 2013). However, the majority of the fill of valley systems consists of a relatively complete record of deposition during the lowstand and early transgressive system tracts, whereby slowly rising sea level locally reduces the fluvial gradient close to the valley shoreline and encourages accumulation (Posamentier and Allen, 1999; Blum and Törnqvist, 2000; Holbrook et al., 2006; Blum et al., 2013). Thus, the sedimentary fill of these types of valleys might provide critical information about earth-surface processes, related depositional history, and its controls, such as the rate of relative sea-level change and its effects on sediment distribution and depositional environments (Posamentier and Vail, 1988; Wright and Marriott, 1993; Shanley and McCabe, 1994; Dalrymple et al. 1994; Zaitlin et al., 1994; Legarreta and Uliana, 1998; Blum et al., 2013). Furthermore, incised-valley systems play key roles in transferring sediments from hinterland regions to deep-marine environments during lowstands, which makes them a useful reference for exploration of sediment linkages to down-dip, coarse-grained lowstand deltas or basin-floor fans (Mitchum 1985; Van Wagoner et al., 1988, 1990; Posamentier, 2001; Törnqvist et al., 2006; Blum and Törnqvist, 2000). Typically, incised valleys are initially filled with coarse-grained fluvial deposits at their base during relative sea-level fall and lowstand, and are subsequently filled by estuarine and marine deposits during the following sea-level rise (Roy, 1984; Dalrymple et al., 1992; Allen and Posamentier, 1993; Wright and Marriott, 1993; Shanley and McCabe, 1993, 1994; Dalrymple et al. 1994; Zaitlin et al., 1994; Blum and Törnqvist, 2000; Blum et al., 2013). Thus, many valley fills are sand prone, which makes them potential hydrocarbon reservoirs and groundwater aquifers (Wright and Marriott, 1993; Shanley and McCabe, 1994; Dalrymple et al. 1994; Zaitlin et al., 1994; Blum et al., 2013), and possible sources of sand for beach renourishment.

Extensive research has been undertaken previously to characterize the internal fill of near-shore incised valleys (e.g., Fisk, 1944; Zaitlin et al., 1994; Wright and Marriott, 1993; Allen and Posamentier, 1993; Shanley and McCabe, 1994; Dalrymple et al., 1994, 2006; Legarreta and Uliana, 1998; Blum et al., 2013). Numerous conceptual, numerical and experimental models have been devised, and scaling relationships identified from modern or ancient case studies, to investigate mechanisms of fluvial channel incision, lateral migration and associated drivers over short timescales ($< 10^3$ yr) (e.g. Hooke, 1979, 1980; Nanson and Hickin, 1983; Fielding and Crane, 1987; Bridge and Mackey, 1993; Mackey and Bridge, 1995; Lawler et al., 1999; Richard et al., 2005; Shanley, 2004; Fielding et al., 2006; Gibling 2006; Blum et al., 2013). However, only a limited number of studies have hitherto focused on geological controls that determine the geometry of near-shore incised valleys and their fills; the results of such studies largely consist of conceptual, experimental, or numerical models (Talling, 1998; Posamentier

and Allen, 1999; Strong and Paola, 2006, 2008; Martin et al., 2011), or are based on case studies of individual incised-valley systems (e.g. Posamentier, 2001; Weber et al., 2004; Ishihara and Sugai, 2017) or of multiple valley systems in a single region (e.g. Mattheus 2007; Mattheus and Rodriguez, 2011; Phillips, 2011; Chaumillon et al., 2008).

In this study, a database-driven statistical analysis has been performed with the aim to investigate the geological controls on the geometry of incised-valley fills. The study is based on a compilation of late-Quaternary incised-valley fills, especially – but not only – those formed during the last glacio-eustatic cycle; the studied examples are representative of different climatic and tectonic settings, and are distributed globally. By restricting the scope of investigation to late-Quaternary examples, the controlling factors on valley characteristics and evolution can be constrained closely. It is therefore possible to relate valley-fill geometry to magnitude of sea-level change, drainage-basin size, drainage-basin vegetation type, physiography of the receiving basin, climate, substrate lithology and tectonics. These variables are generally poorly constrained for most ancient successions. Specific objectives of this work are as follows: (i) to gain an improved understanding of geological controls on valley-fill dimensions; (ii) to evaluate the relative roles of different controls on valley incision and widening; (iii) to present implications of the results for sequence stratigraphy and for hydrocarbon-reservoir prediction and characterization.

BACKGROUND

Observations from experiments (Strong and Paola, 2006, 2008) and investigation of late-Quaternary incised valleys, such as those along the Texas coastal plain (Blum and Price, 1998; Blum et al., 2013), reveal the diachronous nature of the basal surfaces of incised-valley fills; these surfaces do not typically represent relict geomorphic surfaces, but rather amalgamated erosional features resulting from multiple episodes of punctuated channel incisions accompanied by lateral migration, channel-belt deposition and valley-wall reshaping during relative sea-level fall and lowstand. Valley deepening is driven by vertical channel incision, whereas valley widening is largely driven by lateral migration of channels and valley sidewall destabilization (Strong and Paola, 2006, 2008; Martin et al., 2011; Blum et al., 2013). Insight on controls that govern channel incision and lateral migration during relative sea-level fall and rise is therefore useful for exploring the geological controls on incised-valley-fill dimensions. Process-based studies argue that along the continental margins, fluvial incision initiates when a steeper-gradient surface with respect to the fluvial equilibrium profile is exposed during relative sea-level fall (Summerfield, 1985; Leckie, 1994; Talling, 1998; Posamentier and Allen, 1999; Blum and Törnqvist, 2000; Holbrook et al., 2006; Blum et al., 2013). The onset of incision generally occurs at the highstand coastline or at the shelf-slope break when exposed by sea-level fall. Fluvial systems tend to reach their graded profile by landward propagation of retreating knickpoints (Summerfield, 1985; Posamentier and Allen, 1999; Blum and Törnqvist, 2000; Holbrook et al., 2006). Knickpoint migration rates have been shown to be strongly controlled by water discharge (Schumm et al., 1984; Loget and Van Den Driessche, 2009) and substrate characteristics (Van Heijst and Postma, 2001; Loget and Van Den Driessche, 2009). Thus, both the magnitude of sea-level fall and the physiography of the basin determine the largest vertical adjustment of a river system through valley incision, whereas water discharge and substrate characteristics dominate the degree to which, and rate at which, fluvial systems approach the equilibrium profile (Paola et al., 1992). However, rivers might not incise during relative sea-level fall if the shelf is broad and of a gradient similar to, or less than, that of the adjacent coastal plain, and if water discharge is relatively small (cf. Woolfe et al., 1998). Valley downcutting might also take place under conditions of marine transgression, for example because of tectonic and isostatic uplift

of coastal plains, or due to rapid coastal erosion by waves and longshore drift (cf. Leckie 1994). Channel lateral migration rates have been shown to be strongly controlled by water discharge (Hooke, 1979, 1980; Nanson and Hickin, 1983; Lawler et al., 1999; Richard et al., 2005), sediment supply (Sheets et al., 2002; Peakall et al., 2007; Braudrick et al., 2009; Martin et al., 2011), bed material size (Nanson and Hickin, 1986; Richard et al., 2005) and bank stability (Hickin and Nanson, 1975; Nanson and Hickin 1983; Hickin and Nanson, 1984; Lawler et al., 1999; Richard et al., 2005).

Many authors have summarized the fundamental controlling factors that govern valley geometry; principal among these are the rate and magnitude of base-level fall, basin physiography (gradients along the depositional profile and shelf-break depth), climate, substrate characteristics and tectonics (Schumm, 1993; Talling, 1998; Posamentier and Allen, 1999; Holbrook and Schumm, 1999; Blum and Törnqvist, 2000; Posamentier, 2001; Van Heijst and Postma, 2001; Gibling 2006; Strong and Paola, 2006, 2008; Loget and Van Den Driessche, 2009; Martin et al., 2011; Blum et al., 2013).

A number of studies have concentrated on the impact of relative sea-level fall on the formation and morphology of incised valleys (Blum and Törnqvist, 2000; Strong and Paola, 2006, 2008; Martin et al., 2011; Blum et al., 2013). Strong and Paola (2006, 2008) explored the evolution in valley morphology and the emergence of stratigraphic feedbacks in response to relative sea-level fall through experiments that included (i) an isolated slow cycle, where 'slow' is defined with respect to a theoretical equilibrium time that is direct function of basin length (Paola et al., 1992), (ii) an isolated rapid cycle, and (iii) several superimposed rapid cycles, given steady passive-margin style subsidence and constant sediment and water supplies. Physical experiments by Strong and Paola (2006, 2008) indicate that relatively slow sea-level fall could lead to the formation of broader and flatter erosional surfaces, whereas relatively rapid sea-level fall tends to encourage the development of deeper incised valley systems. The same authors also demonstrate that the magnitude of relative sea-level fall primarily determines the valley depth, whereas the rate of relative sea-level fall is a fundamental control on valley width by controlling the duration of time over which the valley-fill boundaries can be shaped. Based on observations from experiments, numerical modelling and field data, Martin et al. (2011) focused on the downstream changes in valley dimensions, indicating that valley width and valley depth tend to increase downstream towards the shoreline position at the beginning of base-level fall, and interpreting such downstream valley widening as related to increased sediment influx from valley excavation, acting independently from relative sea-level changes or initial surface topography. Furthermore, Martin et al. (2011) highlight that both valley depth and valley width increase with the magnitude of relative base-level fall, and that valley widening closely follows valley incision and extension temporally during relative sea-level fall.

The physiography of the depositional profile over which incised valleys develop has been shown to play an important role in valley incision and widening (Summerfield, 1985; Talling, 1998; Posamentier and Allen, 1999; Posamentier, 2001; Blum and Törnqvist, 2000; Törnqvist et al., 2006; Blum et al., 2013). Along the continental margins, the onset of valley incision tends to commence when a convex-up topography is exposed during relative sea-level fall (Summerfield, 1985; Talling, 1998; Blum and Törnqvist, 2000; Blum et al., 2013). Such topographic profiles are typical of the highstand coastline and shelf-slope break. Several authors (Talling, 1998; Posamentier and Allen, 1999; Posamentier, 2001; Törnqvist et al., 2006) have argued that when sea level falls below the shelf break, incised valleys will form across the entire shelf. By contrast, when sea level falls but does not expose the shelf break, incised-valley development will be limited to the region of the coastal prism. Based on observations of present-day gradient profiles along passive margins and margins associated with foreland basins, Talling (1998) further illustrates that if the sea level remains above the shelf break,

4

valley incision will be governed primarily by the geometry of the coastal prism and valley incision will tend to increase with the coastal-prism convexity. Moreover, the magnitude of valley incision is expected to increase basinward towards the highstand shoreline, and then decrease towards the shelf break; the maximum degree of incision is thought to occur at the highstand shoreline (Talling, 1998).

Climate is known to control valley morphology and valley-fill dimensions in a complex manner. It dictates the supply of water and sediment to a river, mediated by effects on variables such as temperature, precipitation, vegetation, and presence of permafrost, particularly through their influence on surface runoff characteristics, which are themselves related to the magnitude and frequency of floods (Blum et al., 1994; Blum and Törnqvist, 2000; Bogaart et al., 2003a, b; Vandenberghe, 2003; Blum et al., 2013). Through analysis of the geometry of late-Quaternary incised-valley systems along the passive continental margins of the northern Gulf of Mexico and of the US mid-Atlantic coast, Mattheus et al. (2007), Mattheus and Rodriguez (2011) and Phillips (2011) show that valley dimensions (valley depth, width and cross-sectional area) are primarily controlled by their drainage-basin area, which is a proxy for the water discharge of their formative rivers; shelf-break depth and coastal-plain and shelf gradients are secondary controls.

Tectonic processes also control valley dimensions, notably through their influence on relative sea-level changes, basin physiography and sediment delivery rates, and indirectly by affecting the drainage-basin climate (Posamentier and Allen, 1999; Jain and Tandon, 2003; Ishihara et al., 2011, 2012; Wohl et al., 2012; Tropeano et al., 2013; Vandenberghe, 2003; Ishihara and Sugai, 2017). Studies on several palaeovalleys (Sugai and Sugiyama, 1998, 1999; Makinouchi et al., 2006; Ishihara et al., 2012; Ishihara and Sugai, 2017) developed on coastal plains in Japan show that tectonic uplift or subsidence act to enhance or reduce, respectively, the effect of sea-level fall on valley dimensions for a given episode of eustatic sea-level fall; local tectonic uplift is generally associated with well-developed terraces and narrow valley floors, whereas local tectonic subsidence is primarily linked to poorly delineated terraces and wide valley floors.

Additionally, wave or tidal erosion causing ravinement during the transgressive stage of incised valley infilling might greatly modify the dimensions of incised-valley fills (e.g. Lericolais et al., 2001; Mattheus and Rodriguez, 2011; Blum et al., 2013).

Existing conceptual models or experimental studies have tended to focus on consideration of one overarching factor (e.g. relative sea-level change) as a control on the geometry of incised-valley fills, whilst treating other parameters as constant. Yet, this is known not to be the case in natural systems. A more comprehensive assessment of controlling factors on the geometry of incised-valley fills is attempted here by means of a comparison of data from multiple case studies, enabled by a database approach.

METHODOLOGY

To evaluate the relative roles of different geological controls that influence valley incision and widening, in this work a statistical analysis of relationships between late-Quaternary incised-valley fills and parameters that describe their context and controlling factors has been undertaken based on data derived from a literature compilation. Data have been coded in a relational database, the Shallow-Marine Architecture Knowledge Store (SMAKS; Colombera et al., 2016), which stores data on the sedimentary architecture and geomorphic organization of shallow-marine and paralic siliciclastic depositional systems. SMAKS includes quantitative data on geological entities of varied nature and scale, and on their associated depositional systems, which can be classified on multiple parameters (e.g., shelf width, delta catchment area) tied to metadata (e.g., data types, data sources).

This study utilizes data on 151 classified late-Quaternary incised-valley fills, 135 of which developed during the last glacial-interglacial cycle (LGC), and 16 of which are of pre-LGC age. The primary data have been extracted from 67 published literature sources. A detailed account of all the case studies included in this work, their associated bibliographic references and the types of data is reported in Table 1, and the location of the studied incised-valley fills is shown in Fig. 1. The datasets that underpin this work are available as part of the supporting information that is available to download as an accompaniment to this paper (see Supplementary Material).

The importance of controls on valley-fill dimensions has been assessed through (i) comparison of descriptive statistics and associated statistical tests and (ii) determination of correlation between variables, as outlined below.

TABLE 1. Case studies stored in the SMAKS database on late-Quaternary incised-valley fills. The table illustrates published literature sources, data types and the age of formation (as LGC or pre-LGC) for each case study. Case-study identification numbers (ID) relate to those coded in the SMAKS database and are referred to in following figures. N = number of incised-valley-fill elements developed for each case study, at or before the LGC.

ID	Case study	Data source	Data types	N	Age
31	Composite database, Gulf of mexico and Atlantic Ocean, USA	Mattheus and Rodriguez (2011); Mattheus et al. (2007)	Airborne images, Cores, Well cuttings, Shallow seismics	38	LGC
38	Pilong Formation, South China Sea, Sunda Shelf	Alqahtani et al. (2015)	Cores, 3D seismics, Shallow seismics	1	LGC
39	Late Quaternary of Manfredonia Gulf, Adriatic Sea	Maselli andTrincardi (2013); Maselli et al. (2014)	Cores, Shallow seismics	1	LGC
42	Lower Tagus Valley, Portugal	Vis et al. (2008); Vis and Kasse (2009)	Cores	1	LGC
44	Rio Grande do Sul, Atlantic coast, Brazil	Weschenfelder et al. (2014)	Cores, Shallow seismics	2	LGC
48	New Jersey shelf, USA	Nordfjord et al. (2005); Nordfjord et al. (2006)	Cores, Shallow seismics	2	LGC
49	Hervey Bay, Queensland, Australia	Payenberg et al. (2006)	Shallow seismics, Bathymetric profile	1	LGC
51	Gulf of Lion, France	Labaune et al.(2005); Labaune et al.(2010); Tesson et al.(2011)	Cores, Shallow seismics	1 / 5	LGC / Pre-LGC
59	Bay of Biscay, France	Weber et al.(2004)	Cores, Shallow seismics	3	LGC
60	Bay of Biscay, France	Proust et al. (2010)	Cores, Shallow seismics	4	LGC
61	Bay of Biscay, France	Chaumillonand Weber (2006)	Cores, Shallow seismics	1	LGC
62	Bay of Biscay, France	Menier et al. (2006)	Cores, Shallow seismics	5	LGC
63	Gulf of Lion, France	Tesson et al. (2015)	Cores, Shallow seismics	3	LGC

65	Late Quaternary of Moreton Bay, Queensland, Australia	Lockhart et al. (1996)	Cores, Shallow seismics	4	LGC
67	Pleistocene of Pattani Basin, South China Sea, Gulf of Thailand	Reijenstein et al. (2011)	Well cuttings, 3D seismics, Shallow seismics	2	Pre-LGC
68	Pilong Formation, South China Sea, Gulf of Thailand	Miall (2002)	3D seismics	1	Pre-LGC
69	Pleistocene of southern Java Sea	Posamentier (2001)	Cores, 3D seismics, Shallow seismics	1	LGC
70	Gironde incised valley, France	Allen and Posamentier (1993); Lericolais et al. (2001)	Cores, Shallow seismics	1	LGC
71	Mekong incised valley, Vietnam	Tjallingii et al. (2010)	Cores, Shallow seismics	1	LGC
72	Late Quaternary of Tuscany, Italy	Amorosi et al. (2013); Rossi et al. (2017)	Cores	3	LGC
73	Ombrone incised valley, Italy	Bellotti et al. (2004); Breda et al.(2016)	Cores	1	LGC
74	Volturno incised valley, Italy	Amorosi et al. (2012)	Cores	1	LGC
75	Biferno incised valleys, Italy	Amorosi et al. (2016)	Cores	1	LGC
				2	Pre-LGC
76	Tiber Delta, Italy	Milli et al. (2013); Milli et al. (2016)	Cores	1	LGC
77	Metaponto coastal plain, Italy	Tropeano et al. (2013)	Cores, Shallow seismics	3	LGC
78	Assu incised valley, Brazil	Gomes et al. (2016)	Shallow seismics	1	LGC
79	Apodi-Mossoró incised valley, Brazil	Vital et al. (2010)	Shallow seismics	1	LGC
80	South Sea of Korea	Lee et al. (2017)	Cores, Shallow seismics	3	LGC
81	KwaZulu-Natal shelf, South Africa	Green (2009); Benallack et al. (2016)	Cores, Shallow seismics	5	LGC
82	Gulf of Papua, Papua New Guinea	Crockett et al. (2008); Daniell (2008)	Cores, Shallow seismics, Bathymetric profile	3	LGC
83	East China Sea	Li et al. (2002); Li et al. (2006); Wellner and Bartek (2003); Zhang and Li (1996); Zhang et al.(2017)	Cores, Shallow seismics	4	LGC
84	Pearl River incised valleys, South China Sea	Li et al. (2006)	Cores	1	LGC
85	Kanto Plain incised valleys, Japan	Ishihara and Sugai (2017); Ishihara et al. (2012)	Cores	3	LGC
86	Pearl River incised valleys, South China Sea	Zhuo et al. (2015)	Cores, Shallow seismics	5	LGC

| 87	Mahakam Delta, Indonesia	Sydow (1996); Roberts and Sydow (2003); Crumeyrolle and Renaud (2003)	Cores, 2D seismics, 3D seismics, Shallow seismics	2	LGC
92	KwaZulu-Natal shelf, South Africa	Green and Garlick (2011)	Shallow seismics	6	LGC
93	Maputo Bay, Mozambique	Green et al. (2015)	Cores, Shallow seismics	3	LGC
94	Cameroon shelf	Ngueutchoua and Giresse (2010)	Cores, Shallow seismics	2	LGC
95	Kosi Bay, South Africa	Cooper et al.(2012)	Cores, Shallow seismics	1	LGC
98	Oregon-Washington shelf, USA	Twichell et al. (2010)	Cores, Shallow seismics, Bathymetric profile	2	LGC
99	Virginia shelf, USA	Colman and Mixon (1988); Colman et al. (1990); Foyle and Oertel (1992); Foyle and Oertel (1997); Oertel and Foyle (1995); Shideler et al. (1984)	Cores, Shallow seismics	1 3	LGC Pre-LGC
100	Parnaíba incised valleys, Brazil	Aquino da Silva et al. (2016)	Shallow seismics	5	LGC
101	Western continental margin of India	Karisiddaiah et al. (2002)	Shallow seismics, Bathymetric profile	1	LGC
103	Chukchi shelf, Alaska, USA	Hill et al. (2007); Hill and Driscoll (2008); Stockmaster (2017)	Cores, Shallow seismics	3 3	LGC Pre-LGC
104	Santa Catarina coast, Brazil	Cooper et al. (2016)	Cores, Shallow seismics	1	LGC
109	Gulf of Cádiz shelf, Iberian peninsula	Lobo et al. (2001); Gonzalez et al. (2004); Lobo et al. (2018)	Shallow seismics, Surface sediment samples	2	LGC
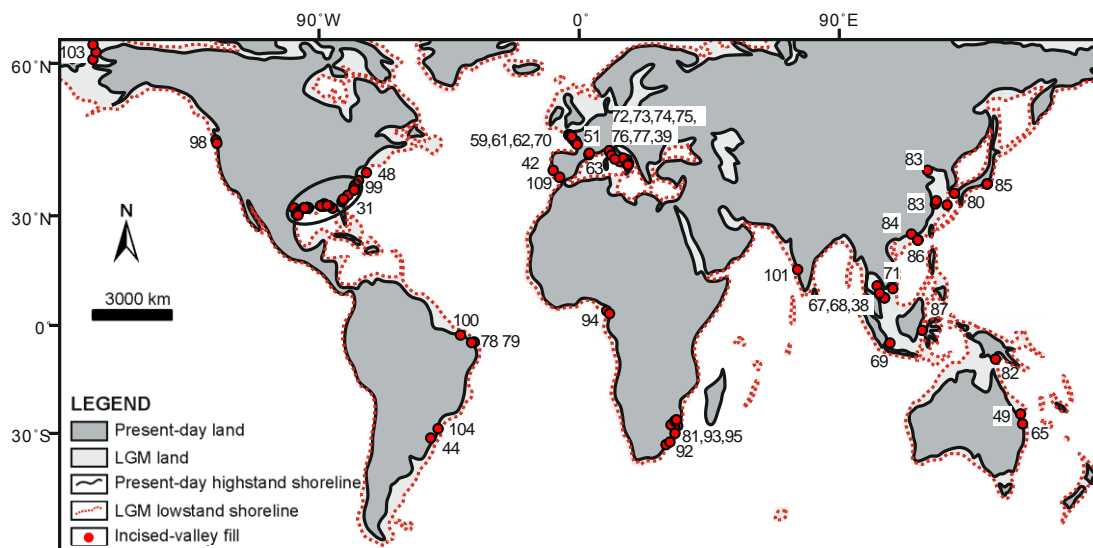
Fig. 1. Location of studied late-Quaternary incised-valley fills. The numbers on the map correspond to the IDs in Table 1. Base map modified from Ray and Adams (2011).

Incised-valley-fill dimensions

In this study, an incised valley is defined as a fluvially eroded, elongate topographic low that is typically larger than a single channel and is generally associated with the juxtaposition of fluvial or estuarine strata on marine deposits and subaerial exposure on interfluves (Van Wagoner et al., 1990; Boyd et al., 2006; Blum et al., 2013). In the original sources, some aggradational channel belts or even channel fills might have been misinterpreted as incised-valley fills. This study avoids inclusion of channel belts or channel fills representing river propagation on the shelf or on shelf-edge deltas at lowstand (Fig. 2C). However, a small number of cases (e.g., Posamentier, 2001; Zhuo et al., 2015; Aquino da Silva et al., 2016), where ambiguity as to the classification of the described successions remains, have been included in the database. Incised-valley geometries vary along dip (Strong and Paola, 2008; Martin et al., 2011; Phillips, 2011). Thus, to enable meaningful comparisons, measurements must be made at the same respective location along the valley axis, to ensure a similar duration of subaerial exposure and record of fluvial and marine processes. In this work valley fills have been classified with respect to the position where their geometry has been characterized, i.e., beneath the present-day coastal plain, on the inner shelf or on the outer shelf. Here, the distinction between inner and outer shelf is made on bathymetry, rather than process regime: the term 'inner shelf' refers to the part of the shelf that extends from the present-day shoreline to the 25 m isobath, whereas the term 'outer shelf' refers to the part of the shelf that extends from the 25 m isobath to the shelf break. Coastal-plain valley fills and inner-shelf valley fills are grouped when analysing the relationships between coastal-plain gradient or coastal-prism convexity versus valley-fill dimensions; inner and outer-shelf valley fills are instead grouped as cross-shelf valleys to assess the relationships between shelf-break depth, shelf width, or shelf gradient versus valley-fill dimensions. This was done to account for the positions where the geometry of incised valleys is expected to be more significantly affected by said controls, as the highstand coastal-prism convexity should control the geometry of valleys carved on the coastal prism, whereas the shelf physiography is predicted to control particularly, although not exclusively, the development of cross-shelf valleys. Only valley fills that represent the products of a single cycle of incision and fill are considered in the subsequent analyses. Compound valley fills that record multiple episodes of incisions and fills, associated with different eustatic cycles, and that thus possess a highly time-transgressive basal surface composed of several amalgamated unconformities, have not been included in this study (cf. Korus et al., 2008). It is also desirable to compare incised-valley fills formed during the same sea-level cycle to account for the effects of the magnitude in sea-level fall on valley dimensions. Here, late-Quaternary incised-valley fills formed during different sea-level cycles are compared, but those associated with the last glacio-eustatic cycle are differentiated and represent the majority of studied examples (135 of 151 valley fills studied; 89%).

The surfaces that should be taken as the boundaries of incised-valley fills have been the subject of debate (Catuneanu et al., 2009). Some authors consider the base of incised-valley fills to represent part of the subaerial unconformity that form sequence boundaries (cf. Helland-Hansen and Martinsen, 1996). In this thinking, the base of an incised-valley fill is placed at the base of the lowstand systems tract, meaning that older falling-stage deposits are not considered part of the fill of an incised valley. In this perspective, the boundaries of incised-valley fills associated with the last glacial cycle would have developed from the Marine Isotope Stage 2 (MIS 2). In contrast, other workers have assigned deposits accumulated during the falling stage to the fill of the incised valleys (e.g., Posamentier et al., 1992; Kolla et al., 1995; Morton and Suter, 1996), such that all of the MIS 4 and younger deposits would still be contained in the incised-valley fills of the last glacial cycle. Of the 135 studied incised-valley fills related to the last glacial cycle considered herein, 13 include deposits of the falling-stage systems tract,

40 exclude falling-stage deposits, whereas 82 could not be differentiated. Considering units that differ in this way will affect any comparison of their cross-sectional area; instead, comparisons of their thickness and width may not be affected, given the position at which falling-stage deposits are expected to occur (cf. Blum et al., 2013).

Where possible, incised-valley fills are classified on their drainage order (90 of 151 valley fills; 60%), i.e., they are differentiated as trunk valleys that reached the lowstand shoreline versus tributary valleys of variable orders; valley fills known to be the expression of third- or higher-order tributary valleys have not been considered.

Incised-valley-fill dimensions (Table 2) were obtained from the original sources, either derived from the text or measured directly on figures using image-analysis software (ImageJ; Schneider et al., 2012). The morphometric parameters that describe the dimensions of incised-valley fills are represented in Fig. 2A. Valley-fill thicknesses are measured where the body is thickest; in cases for which it is not known whether the thickness is measured relative to the thickest portion of the fill (e.g., in 1D well log sample or core sample), the thickness is reported as 'apparent'. For underfilled valleys, values of 'thickness' include the depth of the relic depressions relative to the valley flanks. Valley-fill widths are measured along strike-oriented transects as the distance between the valley walls. 'Apparent' widths are recorded for measurements that are not perpendicular to the valley-fill axis. Thickness and width measurements are classified as 'partial' or 'unlimited' (sensu Geehan and Underwood, 1993; Fig. 2B) for cases where the position of pinch-out of a valley-fill is unknown at one or both ends (e.g., due to outcrop termination), respectively. When derived from borehole correlations, width measurements are recorded as 'correlated'; for purposes of data analysis and presentation, 'unlimited' and 'correlated' measures are not differentiated. Valley-fill cross-sectional areas are measured as vertical cross-sections across the valley in an orientation perpendicular to its axis. The area is measured as the vertical cross-sectional area subtended by the base and top of the valley fill or the elevation of interfluves for underfilled valleys. Only maximum values of valley-fill thickness, width and cross-sectional area are used in the statistical analysis: apparent and partial or unlimited observations have been discarded. For cases where the 3D geometry of valley fills is well constrained, usually for high-resolution seismic data, the largest values of maximum valley-fill thickness, width and cross-sectional area along the valley reach are chosen. In cases where the entire 3D geometry of a valley fill is not known and its downdip variability is not constrained, the largest values of all parameters within the studied sample are recorded, and the observations are classified as located on the shelf or at the highstand coastal prism.

TABLE 2. Parameters that describe the dimensions of incised-valley fills. T: incised-valley-fill thickness; W: incised-valley-fill width; A: incised-valley-fill cross-sectional area. IVF denotes incised-valley fill.

| Parameter	Definition
T (m)	The thickness from the deepest part of the valley axis to the top of the valley fill or the elevation of interfluves for underfilled valleys.
W (m)	Horizontal distance between the valley walls, measured perpendicular to the valley axis.
A (m^2)	The vertical cross-sectional area subtended by base and top of the valley fill or the elevation of interfluves for underfilled valleys, measured in an orientation perpendicular to the valley axis.
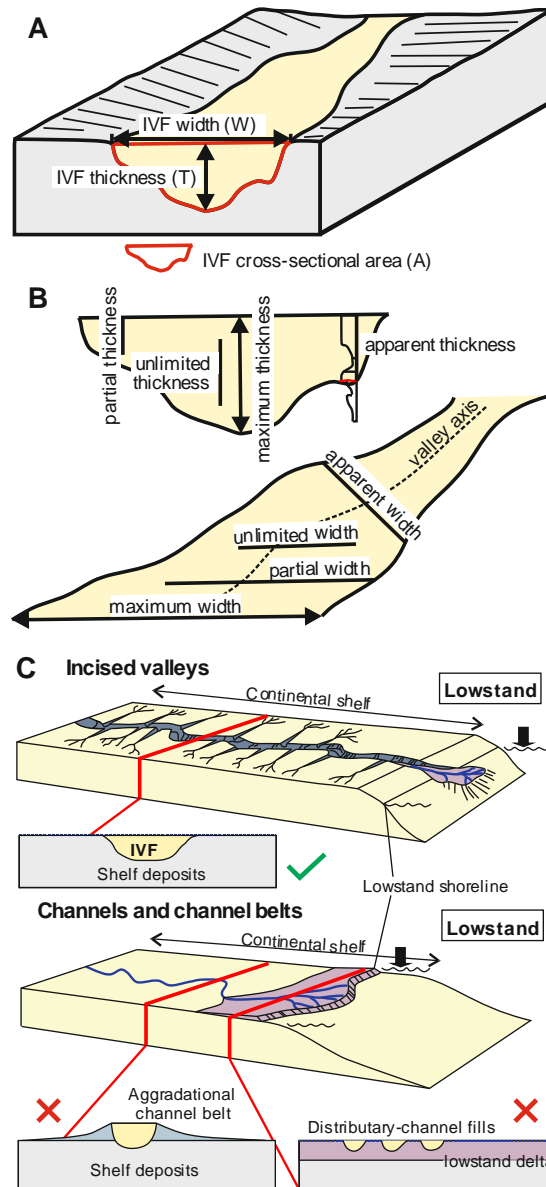
Fig. 2. (A) Incised-valley-fill dimensions (incised-valley-fill thickness, width and cross-sectional area) measured in our analysis. (B) Classification of incised-valley-fill thickness and width by type of observation, i.e., as 'maximum', 'apparent', 'partial' and 'unlimited' (see text). (C) Diagram illustrating channel belts associated with river propagation on the shelf at lowstand and distributary channels associated with lowstand deltas, neither of which are included in this study.

Quantification of basin physiography

In this study, the present-day physiography of the shelf and subaerial nearshore has been taken as a proxy for the physiography of the continental shelf and nearshore during the Last Interglacial (LI) highstand (Fig.3). However, this assumption carries significant uncertainty due to potential differences in basin physiography between the present and the LI, likely arising from spatial variations in isostatic adjustment, spatial variations in post-glacial shelf and shelf-break accretion, differences in process regime, variable styles of fluvial and shoreline responses expected in different climatic and tectonic settings, and because of autogenic dynamics. Present-day lower-coastal-plain gradients (Fig. 3) have

11

been measured perpendicular to the orientation of the present-day shoreline along a 10-km transect landward of the shore, utilizing digital elevation data from Becker et al. (2009). Gradients have also been calculated for the tract of subaqueous nearshore that extends from the shoreline to 25-m isobath, as representative values of inner-shelf gradients (Fig. 3), using digital bathymetric data by Becker et al. (2009). The difference in gradient between present-day lower coastal plains and inner shelves is taken as a measure of the convexity of the present-day coastal prism (Fig. 3; Table 3). The shelf-break depth is measured at the shelf-break location mapped by Harris et al. (2014), using digital bathymetric data by Becker et al. (2009). The shelf width is measured as the distance from the present-day shoreline to the shelf break, as mapped by Harris et al. (2014). For cases in which the shoreline is irregular and does not mirror the orientation of the shelf break, the length along the valley axis from the present-day shoreline to the shelf break is recorded as an additional attribute.

TABLE 3. Parameters used to describe the settings of the studied incised-valley fills. CPG10: lower-coastal-plain gradient; ISG25: inner-shelf gradient; CPC: coastal-prism convexity; SBD: shelf-break depth; SW: shelf width; SDL: the length from the shoreline to the shelf break; SG: shelf gradient; L: latitude; DBA: drainage-basin area.

Parameter	Definition
CPG10 (°)	The mean gradient measured perpendicular to the shoreline along a 10-km transect landward of the present-day shoreline, in degrees.
ISG25 (°)	The mean gradient measured from the present-day shoreline to the 25-m isobath in an offshore direction, in degrees.
CPC (°)	The difference in gradient between present-day lower coastal plains and inner shelves, in degrees.
SBD (m)	Depth of the shelf break.
SW (km)	The horizontal distance between the present-day shoreline and the shelf break.
SDL (km)	The length along the valley axis from the present-day shoreline to the shelf break.
SG (°)	The mean gradient of the shelf between the present-day shoreline and the shelf break, in degrees.
L (°)	The absolute value of the latitude of the location where the incised-valley fill has been measured.
DBA (km^2)	Area of the drainage-basin catchments feeding the incised valley at lowstand, landward of the location where the incised-valley fill has been measured.

Drainage-basin size

The drainage-basin size has been determined based on the catchment area landward of the location where the incised-valley-fill geometry was measured. For valley systems whose drainage networks during the Last Glacial Maximum (LGM) have been reconstructed and presented in the scientific literature, drainage areas were measured at the location where the incised-valley fills were characterized. In other cases, the river systems that contributed to the lowstand drainage network of incised valleys now buried under coastal plains can be reconstructed confidently; in these cases

estimations based on catchment areas of present-day rivers have been considered as the sum of all different drainage basins that are inferred to have amalgamated at lowstand, as shown in Fig. 4.
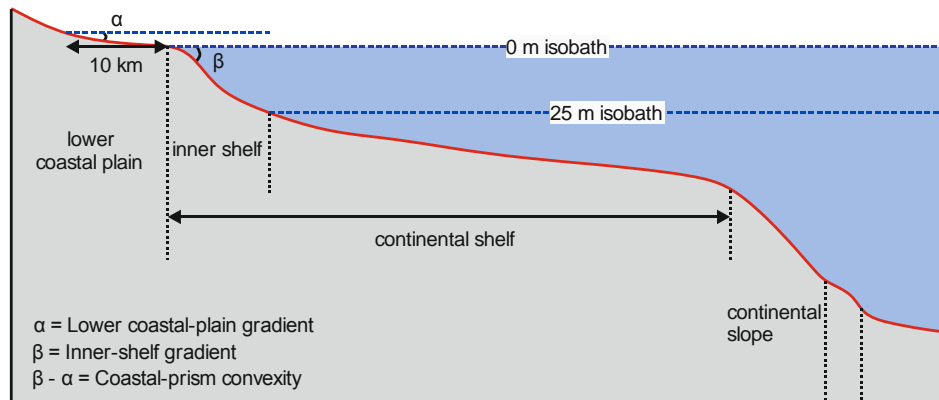

Fig. 3. Definition sketch of the physiography of the depositional profile over which incised valleys develop.
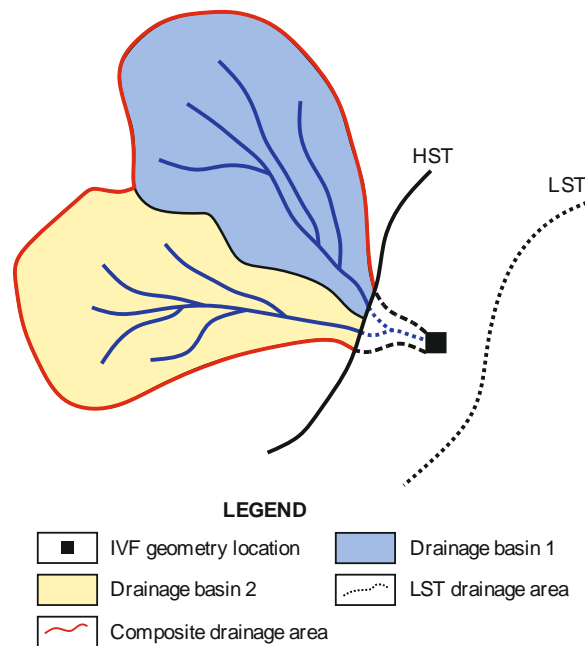

Fig. 4. Schematic diagram illustrating the measurement of contributing drainage-basin area corresponding to each incised-valley fill. HST denotes the highstand coastal shoreline (present-day shoreline) and LST denotes the lowstand shoreline (e.g., LGM shoreline).

LGM catchment vegetation

The global distribution of dominant vegetation types during the LGM has been mapped by Ray and Adams (2011), based on plant-fossil data and proxy zoological and sedimentologic data. Based on the map by Ray and Adams (2011), the proportionally most prevalent type of vegetation in the catchment area was recorded for each incised-valley fill. Vegetation types were recorded in terms of two

alternative schemes (i.e., one including classes: 'forest', 'grassland or woodland', 'desert'; the other including classes: 'tropical or subtropical', 'temperate', 'polar or subpolar').

Statistical analyses

Statistical analyses have been performed to determine relationships between variables and to test hypotheses relating to differences in means across populations. For pairs of continuous variables, Pearson or Spearman correlation coefficients (denoted with R and r hereafter) are respectively used to quantify linear and monotonic relationships, whose statistical significance is expressed as p-values (p hereafter). The statistical significance of differences in the mean of variables across groups is determined with a two-sample t-test when dealing with two sets of observations, and with one-way analysis of variance (ANOVA) when dealing with three or more sets of observations. Resulting test statistics (t for t-tests, F for ANOVA) are considered jointly with the number of degrees of freedom (df hereafter) to determine the statistical significance of differences across groups, expressed as p-values (p). All statistical analyses were performed in Minitab 17.

RESULTS AND INTERPRETATIONS
Continental-margin type
Observations

The studied late-Quaternary valley fills were classified as hosted on passive, active, and transform margins. Valley fills from transform margins and passive margins are considered together in the subsequent analyses. A comparison has been made of incised-valley fills developed on passive and active continental margins. The thickness, width and cross-sectional area (Fig. 5A-C) of incised-valley fills associated with active margins are, on average, larger than those along passive margins, and the difference is important for values of mean valley-fill thickness (mean(T) = 50.1 versus 28.2 m; mean(W) = 7,099 versus 3,862 m; mean(A) = 200,545 versus 73,200 m^2, respectively). Two-sample t-tests confirm that means in valley-fill morphometric parameters are significantly different in the two settings (t-value= 4.53, p-value < 0.001, df = 16, for T; t-value= 2.40, p-value= 0.030, df = 15, for W; t-value= 2.90, p-value= 0.010, df = 18, for A). Distributions in drainage area for the two margin types (Fig. 5D) show that drainage-basin areas associated with passive margins are larger, on average, than those associated with active margins (mean $DBA_{passive}$ = 60,672 m^2, mean DBA_{active} = 17,012 km^2, 2-sample t-test: t-value= -2.57, p-value= 0.012, df = 76).

Interpretations

Tectonics can significantly influence fluvial incision through a first-order control on basin physiography (Posamentier and Allen, 1999). Tectonically active margins are commonly characterized by the formation of narrow, high-gradient shelves, which favour deep fluvial incision (Schumm and Brakenridge, 1987; Leckie, 1994; Posamentier and Allen, 1999). In contrast, passive margins are characterized by the development of wide, low-gradient shelves, in part because such margins are generally associated with larger drainage-basin areas (Blum et al., 2013), as shown in Fig. 5D, and thus lower-gradient shelves (see below); this in turn is reflected in shallower fluvial incision for base-level falls of given magnitude. Distributions of valley-fill thickness for these two margin types (Fig. 5A) support this expectation. In addition, local tectonic uplift might be experienced by shelves on active margins (Posamentier and Allen, 1999; Ishihara and Sugai, 2017), which would induce fluvial incision (Posamentier and Allen, 1999; Holbrook and Schumm, 1999; Holbrook et al., 2006; Tropeano et al., 2013; Ishihara et al., 2011, 2012; Ishihara and Sugai, 2017). For example, the Metaponto coastal plain in Italy (case study 77 in Table 1) has been experiencing regional uplift since the Middle Pleistocene

(Doglioni et al., 1996; Patacca and Scandone, 2001), at rates varying from 0.3 to 0.9 mm/yr as estimated from dated stranded marine terraces (Cilumbriello et al., 2008, 2010; Caputo et al., 2010; Tropeano et al., 2013). Three incised-valley fills developed beneath the Metaponto coastal plain are characterized by larger-than-average thickness, despite being associated with smaller-than-average drainage areas, as illustrated in Fig. 5A-C.

Incised-valley widening is partly driven by the lateral migration of fluvial channel belts (Martin et al., 2011). Previous work based on experiments, numerical modelling and field studies (Strong and Paola, 2006, 2008; Martin et al., 2011; Blum et al., 2013) have shown that lateral channel migration and channel-belt deposition are closely concomitant with valley incision unless the valley sidewalls are resistant to erosion or the system is starved of sediments, implying that valley widening generally follows valley incision temporally during relative sea-level fall. The examples associated with active margins studied here are all incised into unconsolidated sand-rich coastal or shelf deposits, such that valley-fill width is expected to be scaled with valley-fill thickness.

Furthermore, tectonics also indirectly affects the morphology and behaviour of fluvial systems through orographic control on climate. Regions undergoing rapid uplift are typically associated with high relief, favouring orographic precipitation (Joeckel, 1999; Ruddiman, 2013), which in turn controls water discharge. High elevation river basins draining active margins are characterized by larger runoff per basin area (Milliman and Syvitski, 1992). In addition, tectonically active systems are generally associated with smaller catchments than passive ones (Fig. 5D), such that storms are more likely to affect the entire drainage basin and floods to propagate through the entire channel network (Sømme et al., 2009a). Thus, tectonically active systems associated with small drainage areas ($<10^4$ km^2) are more prone to large differences between flood and base-flow discharge (2 to 3 orders of magnitude; Sømme et al., 2009a). Additionally, active margins tend to have steep gradients throughout the river network (Flint, 1974; Sømme et al., 2009a; Blum et al., 2013), which are expected to control stream power in a way that would promote fluvial incision (Schumm et al., 1984; Paola et al., 1992; Blum et al., 2013) and lateral migration of river channels (Hooke, 1979, 1980; Nanson and Hickin, 1983; Lawler et al., 1999; Richard et al., 2005). Furthermore, active margins are commonly subject to hill-slope destabilization, partly because of seismic triggering (Jain and Tandon, 2003; Wilson et al., 2007). Rivers associated with active margins tend to have greater specific sediment yield and carry a higher proportion of bedload than those associated with passive margins (Milliman and Syvitski, 1992), which in turn favour channel lateral migration and thus valley widening (Dietrich and Whiting, 1989; Sheets at al., 2002; Strong and Paola, 2006, 2008; Peakall et al., 2007; Braudrick et al., 2009; Martin et al., 2011; Blum et al., 2013). Peak water discharge and rates of sediment flux might have been particularly high for incised valleys now infilled in the Kanto plain (Japan) and in Indonesia (case study 85 and 87 in Table 1, respectively), as these areas were subject to tropical monsoonal climate during the LGM (Crowley and North 1991; Broecker 1995; Adams and Faure, 1997; Ray and Adams, 2011).

As a caveat to these results, it must be noted that the distributions of drainage areas for the incised-valley fills considered in this work do not cover the full spectrum of catchment sizes documented for modern rivers (cf. Blum et al. 2013); in particular, the distribution of drainage areas for valley systems on passive margins considered in this work does not encompass those that would correspond with the world's largest river systems. Considering the highly skewed nature of distributions of drainage areas (Fig. 5D), the inclusion of very large valley systems might significantly affect values of maximum size, but less significantly the mean values for which the statistical significance was tested. Notwithstanding, although the data suggest that the type of continental margin is a good predictor of

incised-valley fill geometry, any conjecture on the effective role of specific controlling factors needs to be substantiated with more data.
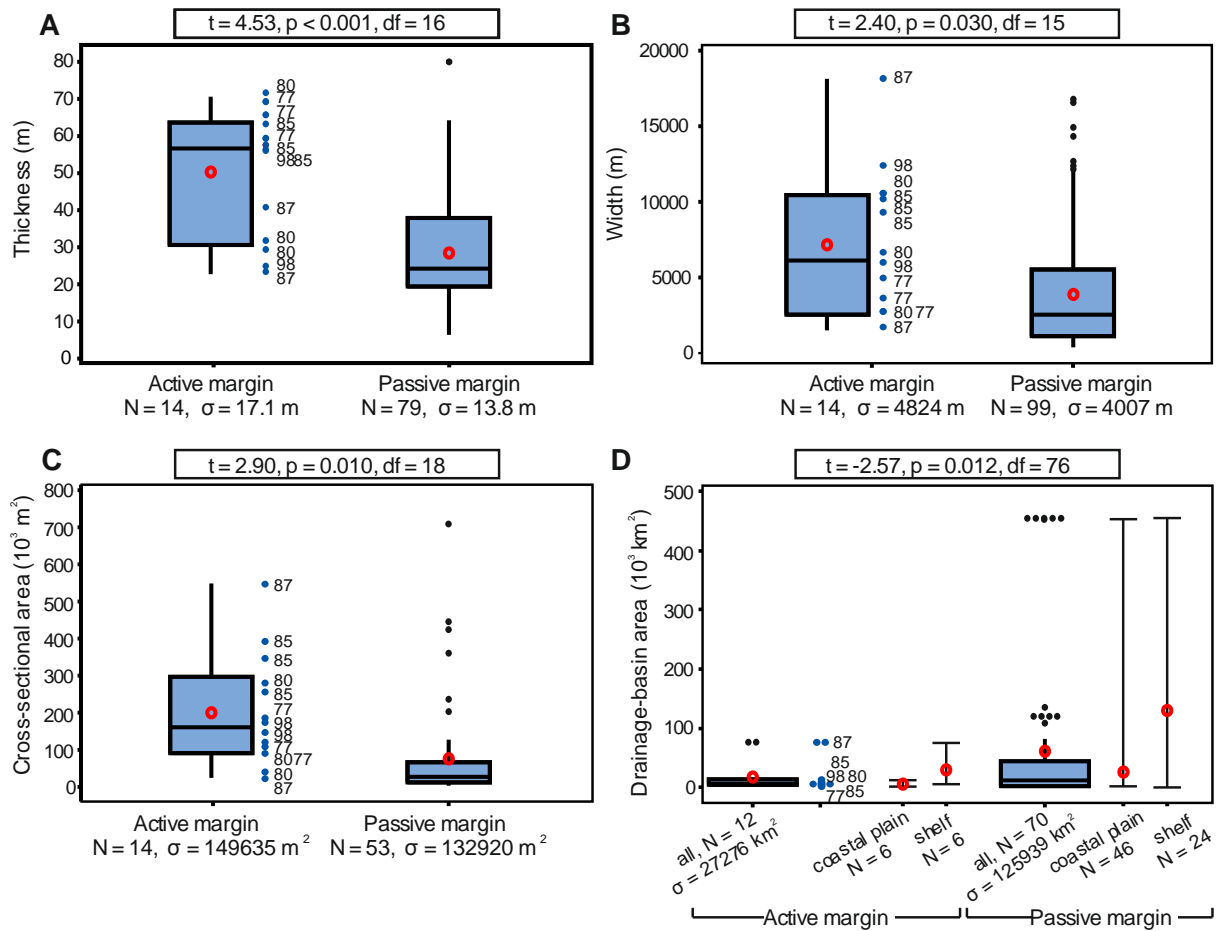

Fig. 5. Box-plots that present distributions in: (A) late-Quaternary incised-valley-fill thickness, (B) width, (C) cross-sectional area, and (D) drainage-basin size, for active and passive continental margins. Individual values are also shown next to the boxplot for active margins and the numerical labels refer to IDs in Table 1. In D, mean and range plots are illustrated near each boxplot for examples hosted on the shelf and coastal plains, respectively. For each boxplot, boxes represent interquartile ranges, red open circles represent mean values, horizontal bars within the boxes represent median values, and black dots represent outliers (values that are more than 1.5 times the interquartile range). 'N' denotes the number of readings and 'σ' denotes the standard deviation. The results of 2-sample t-test (t-value, p-value and df) are reported in respective boxes. 'df' denotes the degrees of freedom.

Basin physiography
Shelf-break depth
Observations

The maximum sea-level lowstand during the LGM was 120 to 130 m below that of present-day levels (Fairbanks, 1989; Yokoyama et al., 2000; Lambeck and Chappell, 2001; Peltier and Fairbanks, 2006; Simms et al., 2007b). However, the magnitude of fall varied geographically and across estimates made by different authors. In the following statistical analysis, to assess distributions in valley-fill dimensions for shelves that were completely or partially exposed at the LGM, different values of shelf-

break depth were considered (120 m, 125 m and 130 m). Similar results were obtained for the three different depths; all results are therefore only presented for the 120-m shelf-break depth threshold. For the LGC examples, incised-valley fills hosted on shelves with shelf-break depth larger than 120 m display greater thickness, width and cross-sectional area, on average (Fig. 6A-C), than those with shelf break shallower than 120 m (mean(T) = 39.1 m versus 27.5 m; mean(W) = 10,519 m versus 4,004 m; mean(A) = 202,033 m^2 versus 78,538 m^2). Two-sample t-tests for valley-fill dimensions in these two scenarios indicate significant differences between the means of these two populations (t-value = -3.30, p-value = 0.001, df = 103, for T; t-value = -2.86, p-value = 0.006, df = 56, for W; t-value = -2.08, p-value = 0.045, df = 37, for A). Valley fills associated with shelves with deeper shelf breaks tend to have larger drainage-basin areas (mean = 216,131 m versus 27,698 m; 2-sample t-test: t-value = -2.66, p-value = 0.011, df = 42) (Fig. 6D).

For cross-shelf valley fills hosted on shelves with shelf break shallower than 120 m (Fig. 7A-C), valley-fill thickness is negatively correlated with shelf-break depth (r = -0.427, p-value = 0.033); no correlation is seen between valley-fill width or cross-sectional area and shelf-break depth (r(W) = 0.085, p-value = 0.693; r(A) = -0.110, p-value = 0.616). For cross-shelf valley fills hosted on shelves with shelf break deeper than 120 m (Fig. 7A-C), a weak correlation is seen between valley-fill width and shelf-break depth (r = 0.335, p-value = 0.032), whereas there is very weak or no correlation between valley-fill thickness or cross-sectional area and shelf-break depth (r(T) = 0.201, p-value = 0.208; r(A) = 0.057, p-value = 0.792).

Interpretations

Previous work based on conceptual models has proposed (Talling, 1998; Posamentier and Allen, 1999; Posamentier, 2001; Törnqvist et al., 2006) that relative sea-level falls that are larger in magnitude than the depth of the shelf break, by resulting in full exposure of the shelf, will drive the formation of incised valleys cutting through the shelf, whereas relative sea-level falls of magnitude lower than the shelf-break depth are expected to lead to the formation of valleys that are mostly confined around the highstand coastal prism. Fluvial systems on shallower shelves are expected to undergo a greater vertical river-profile adjustment, resulting in greater valley incision. However, the data do not fully support this view, as shelves with breaks deeper than 120 m tend to contain larger incised-valley fills. This could be explained by the fact that the studied shelves with shelf breaks that are deeper than 120 m are primarily linked to larger drainage-basin areas, compared to those with shallower shelf breaks (Fig. 6D).

The correlation between valley-fill thickness and shelf-break depth for cross-shelf valley fills hosted on shelves with shelf break shallower than 120 m (Fig. 7A) might indicate a causal link between magnitude of exposure, depth of incision, and resulting valley-fill thickness. However, shelves with deeper shelf breaks tend to have steeper shelf gradients on average, which results in larger differences between the shelf gradient and the fluvial equilibrium profile and therefore should tend to drive deeper fluvial incision for a given relative sea-level fall (Schumm and Brakenridge, 1987; Leckie, 1994; Posamentier and Allen, 1999).
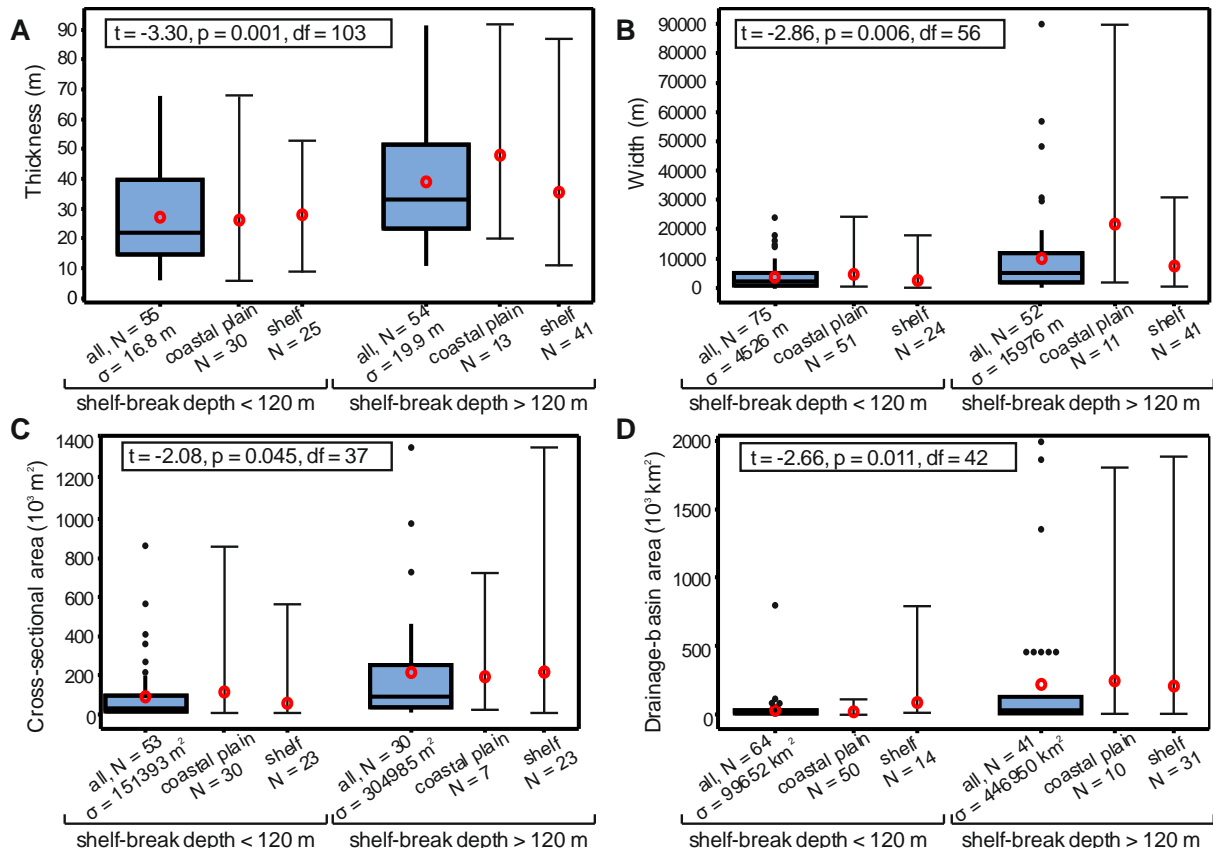
Fig. 6. Box plots and mean/range plots of: (A) LGC incised-valley-fill thickness; (B) width; (C) cross-sectional area; and (D) drainage-basin area distributions for different shelf-break depths, divided by 120 m, which is the magnitude of the fall in eustatic sea-level associated with LGM. Mean and range plots are illustrated near each boxplot for examples hosted on the shelf and coastal plains, respectively. For each boxplot, boxes represent interquartile ranges, red open circles represent mean values, horizontal bars within the boxes represent median values, and black dots represent outliers (values that are more than 1.5 times the interquartile range). For each mean and range plot, red open circles represent mean values and horizontal bars represent the minimum or maximum of all the data. 'N' denotes the number of readings. 'σ' denotes the standard deviation. The results of 2-sample t-test (t-value, p-value and df) are reported in respective boxes. 'df' denotes the degrees of freedom.

Shelf width

Observations

Positive correlations are seen between the width and cross-sectional area of cross-shelf incised-valley fills and the width of the shelf (r(W) = 0.528, p-value < 0.001; r(A) = 0.503, p-value = 0.002) (Fig. 8B and C). No apparent correlation is seen between valley-fill thickness and shelf width (R = 0.078, p-value= 0.593) (Fig. 8A).

Interpretations

Positive relations between the width or cross-sectional area of cross-shelf incised-valley fills versus the width of the shelf (Fig. 8) do not indicate a causal link between shelf width and valley dimensions. Large fluvial basins are generally associated with wider shelves through a control on sediment input and shelf progradation (Burgess and Steel, 2008; Blum and Hattier-Womack, 2009; Olariu and Steel, 2009; Helland-Hansen et al., 2012; Blum et al., 2013). The results might indicate that

shelf width and incised-valley-fill dimensions co-vary in relation to a common control exerted by the size of drainage areas.
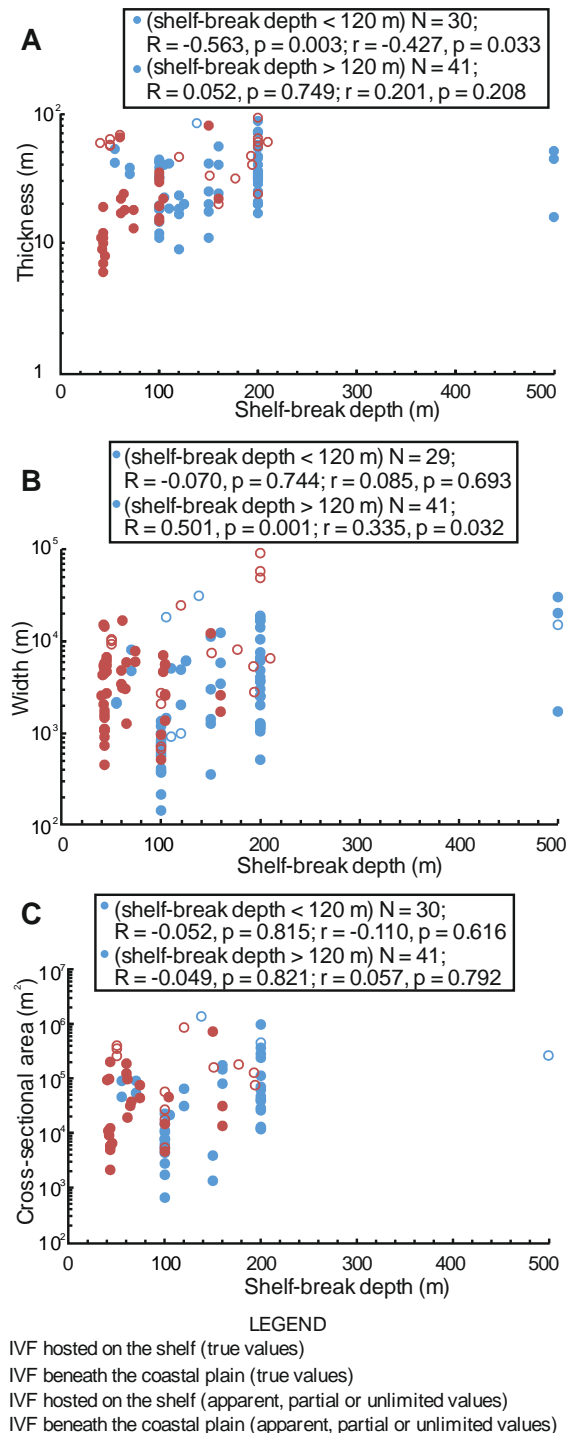

Fig. 7. Plots of: (A) LGC incised-valley-fill thickness; (B) width; and (C) cross-sectional area versus shelf-break depth. For each pair of variables, correlation coefficients and p-values are included in respective boxes for cross-shelf incised-valley fills, and separately reported for shelves with shelf break shallower than 120 m and deeper than 120 m. 'N' denotes the number of readings, 'R' denotes Pearson's R, and 'r' denotes Spearman's rho.
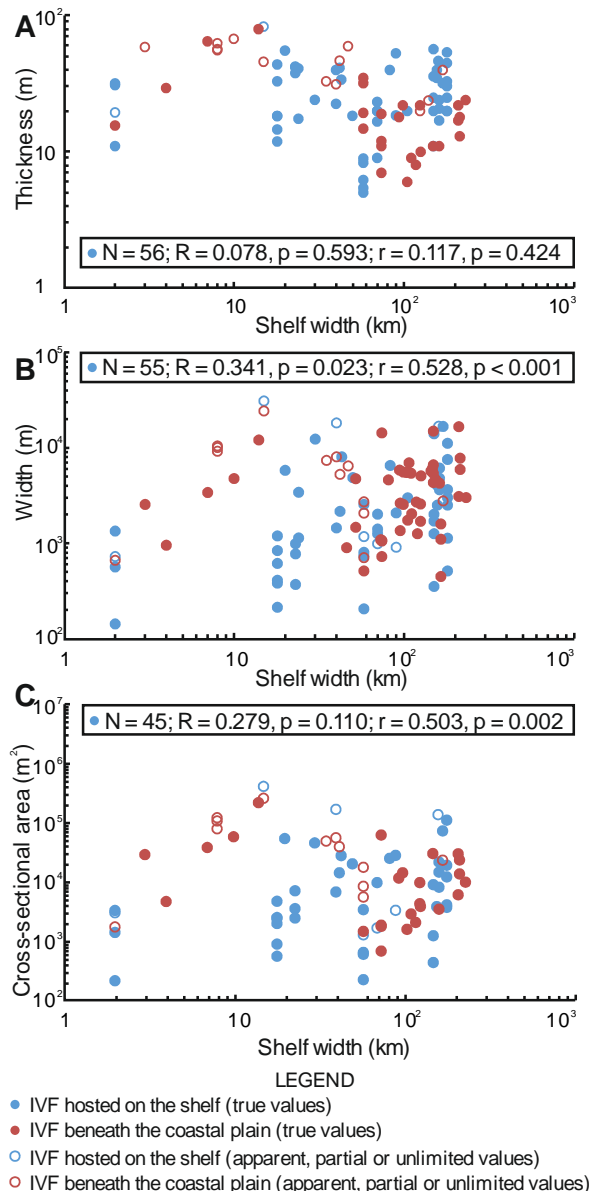
Fig. 8. Plots of: (A) cross-shelf incised-valley-fill thickness; (B) width; and (C) cross-sectional area versus shelf width. For each pair of variables, the correlation coefficients of determination and p-values for cross-shelf valley fills are reported in respective boxes. 'N' denotes the number of readings, 'R' denotes Pearson's R, and 'r' denotes Spearman's rho.

Coastal-plain gradient

Observations

Negative correlations are seen between the width and cross-sectional area of incised-valley fills recognized beneath present-day coastal plains and on the inner shelf versus associated present-day lower coastal-plain gradients ($r(W) = -0.452$, p-value < 0.001; $r(A) = -0.433$, p-value < 0.001) (Fig. 9B and C). No apparent correlation is seen between valley-fill thickness and lower coastal-plain gradients ($r(T) = -0.198$, p-value $= 0.064$) (Fig. 9A). A corresponding negative relationship is seen between drainage-basin area versus coastal-plain gradients ($r = -0.388$, p-value < 0.001) (Fig. 9D).

Interpretations

Negative correlations between the width or cross-sectional area of valley fills versus lower-coastal-plain gradient (Fig. 9) are unlikely to indicate a causal link between coastal-plain gradient and valley dimensions. Rather, they likely reflect the fact that smaller basins feeding smaller rivers tend to be associated with higher gradients at the river mouths, and vice versa (Flint, 1974; Blum et al., 2013), as is also evident in Fig. 9D.
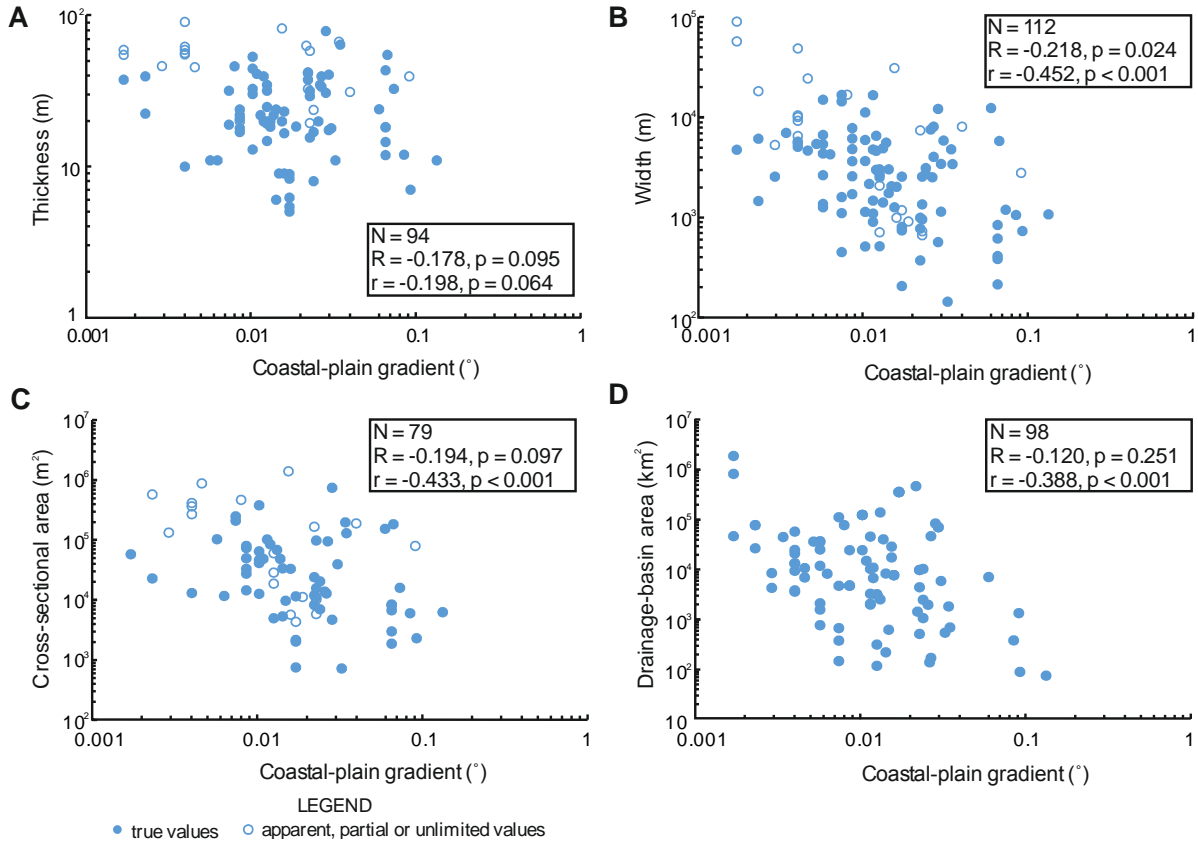

Fig. 9. Plots of: (A) coastal-plain and inner-shelf incised-valley-fill thickness; (B) width; (C) cross-sectional area; and (D) drainage-basin area versus lower coastal-plain gradient. For each pair of variables, the correlation coefficients of determination and p-values are reported in respective boxes. 'N' denotes the number of readings, 'R' denotes Pearson's R, and 'r' denotes Spearman's rho.

Shelf gradient
Observations

For LGC incised-valley fills hosted on the shelf, values of thickness, width and cross-sectional area all tend to decrease with the average shelf gradient (r(T) = -0.255, p-value = 0.043; r(W) = -0.478, p-value < 0.001; r(A) = -0.486, p-value = 0.002) (Fig. 10A-C). A corresponding negative relationship is seen between drainage-basin area and shelf-gradient (Fig. 10D). For incised-valley fills measured beneath the coastal plains (Fig. 10A-D), valley-fill thickness and cross-sectional area are positively correlated with the average shelf gradient (r(T) = 0.582, p-value < 0.001; r(A) = 0.401, p-value = 0.014); there is very weak or no correlation between valley-fill width or drainage-basin area and the average shelf gradient (r(W) = -0.004, p-value = 0.974; r(DBA) = -0.139, p-value = 0.289).

Interpretations

These relations may not indicate a causal link between shelf gradient and cross-shelf valley-fill dimensions. Rather, these results might arise because larger fluvial systems associated with larger drainage basins tend to be associated with shelves with lower gradients, as is also indicated in Fig. 10D. This might be explained by the fact that the gradient of shelves that occur offshore of river-dominated coasts is in part determined by the profile of the rivers traversing it at lowstand, and larger fluvial systems are associated with lower channel gradients (Wood et al., 1993; Burgess and Streel, 2008; Sømme et al., 2009a, b; Blum and Hattier-Womack, 2009; Olariu and Steel, 2009; Helland-Hansen et al., 2012; Blum et al., 2013).

Positive correlations between coastal-plain valley-fill thickness and shelf gradient (Fig. 10A and C) might be attributed to variations in the difference between the gradient of the shelf and the river equilibrium profile (Schumm and Brakenridge, 1987; Leckie, 1994; Posamentier and Allen, 1999).
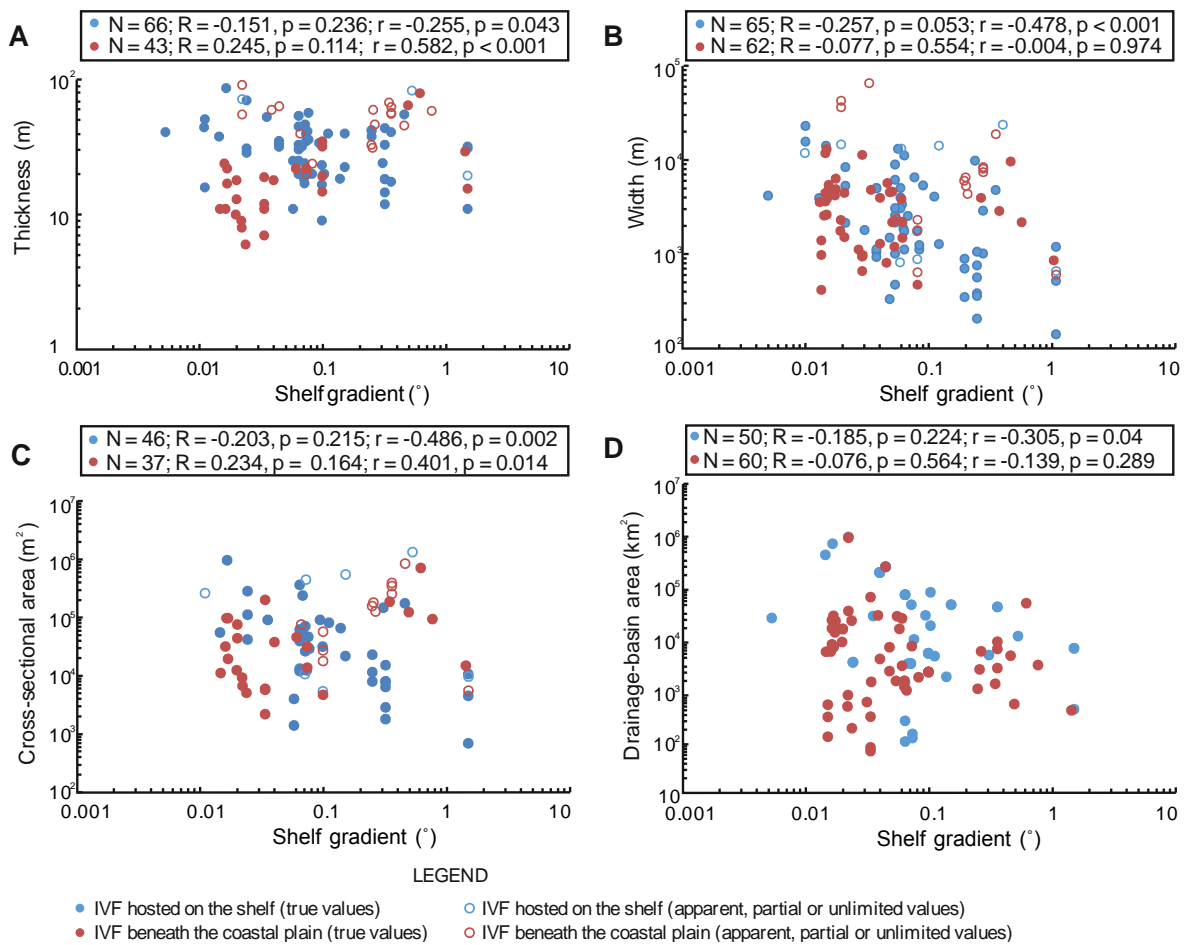
Fig. 10. Plots of: (A) incised-valley-fill thickness; (B) width; (C) cross-sectional area; and (D) drainage-basin area versus shelf gradient. For each pair of variables, the correlation coefficients of determination and p-values for cross-shelf incised-valley fills and valley fills developed beneath the coastal plain are reported in respective boxes. 'N' denotes the number of readings, 'R' denotes Pearson's R, and 'r' denotes Spearman's rho.

Coastal-prism convexity

Observations

In this work, the difference in gradient between present-day lower coastal plains and inner shelves is used as a measure of the convexity of the coastal prism. In order to analyse the relations between coastal-prism convexity and valley-fill dimensions, examples associated with inner shelves that are gentler than the associated lower coastal plains were excluded in this analysis. Fig. 11A-C illustrate that for inner shelves that are steeper than the associated lower coastal plains (127 of 135 valley fills; 94%), moderate negative correlations are seen between incised-valley-fill width and cross-sectional area versus the difference in gradient between present-day inner shelf and coastal plain (r(W) = -0.413, p-value < 0.001; r(A) = -0.255, p-value = 0.034); no correlation is observed between valley-fill thickness and the same gradient difference (r(T) = 0.081, p-value = 0.463).
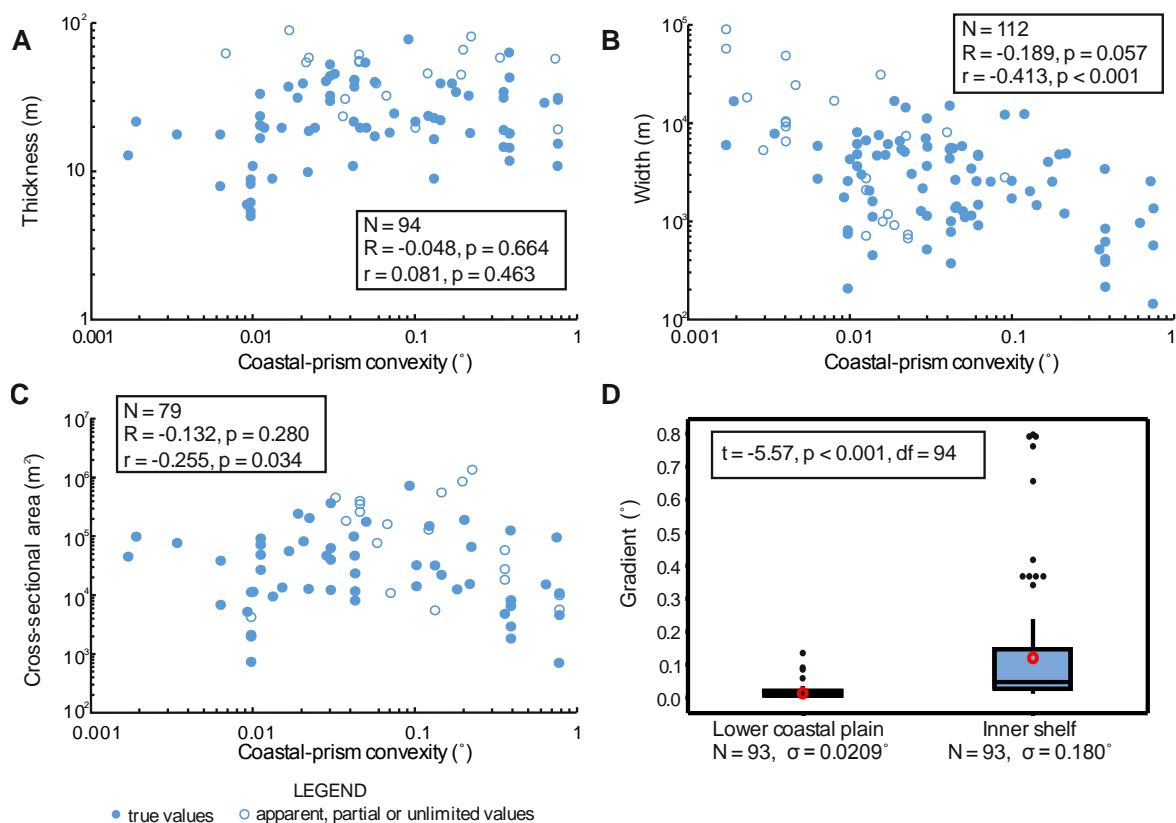

Fig. 11. Plots of: (A) coastal-plain and inner-shelf incised-valley-fill thickness; (B) width and (C) cross-sectional area versus coastal-prism convexity. For each pair of variables, the correlation coefficients of determination and p-values are reported in respective boxes. 'N' denotes the number of readings, 'R' denotes Pearson's R, and 'r' denotes Spearman's rho. (D) Box plots of gradient distributions for lower coastal plains and inner shelves. For each boxplot, boxes represent interquartile ranges, red open circles represent mean values, horizontal bars within the boxes represent median values, and black dots represent outliers (values that are more than 1.5 times the interquartile range). 'N' denotes the number of readings and 'σ' denotes the standard deviation. The results of 2-sample t-test (t-value, p-value and df) are reported in respective boxes. 'df' denotes the degrees of freedom.

Interpretations

The correlations between the difference in gradients and both valley-fill width and cross-sectional area may not indicate a causal link. Inner-shelf gradients vary from 0.0117° to 0.7957° (mean

ISG25 = 0.121°, StDev = 0.180°), which is nearly an order of magnitude larger than the typical gradient of coastal plains (range 0.0017° to 0.0934°, mean CPG10 = 0.0169°, StDev = 0.0209°) (Fig. 11D); the difference in these two gradients might therefore approximate the inner-shelf gradient, and any correlations with the estimated coastal-prism convexity might then merely reflect correlations between shelf gradient and valley-fill width or cross-sectional area (see above).

Some conceptual models (Talling, 1998; Posamentier and Allen, 1999; Posamentier, 2001; Törnqvist et al., 2006) envisage that if the sea level does not fall beyond the shelf break, fully exposing the shelf, magnitude and location of valley incision should primarily be determined by the coastal-prism convexity. However, observations summarised in Fig. 11A contradict this hypothesis. This discrepancy might be due to the influence of overriding factors, or to the fact that the estimates of convexity for present-day costal prisms do not approximate the convexity of the coastal prisms established during the last interglacial.

Drainage-basin characteristics
Drainage-basin size
Observations

Incised-valley-fill thickness, width and cross-sectional area all correlate directly with drainage-basin size (r(T) = 0.348, p-value = 0.001; r(W) = 0.402, p-value < 0.001; r(A) = 0.429, p-value < 0.001) (Fig. 12A-C). For valley fills along passive margins, correlation between valley-fill cross-sectional area and drainage-basin size is stronger (r = 0.706, p-value < 0.001) (Fig. 12C).

Interpretations

Based on statistical analysis of incised valleys from the northern Gulf of Mexico and the mid-Atlantic US margin, Mattheus et al. (2007), Mattheus and Rodriguez (2011) and Phillips (2011) have demonstrated that valley dimensions at comparable locations along valley axis (at the MIS5e shoreline or near the head of the present-day deltaic plain) are strongly correlated to the drainage-basin area, and that for passive continental margins, where the gradient of coastal plains and shelves does not vary significantly, upstream controls such as discharge should play a primary role in determining valley-fill shape and size. Our observations (Fig. 12) support the role of drainage-basin area as important control on incised-valley-fill dimensions, especially for valley fills developed along passive margins. Previous studies (Schumm et al., 1984; Van Heijst and Postma, 2001; Loget and Van Den Driessche, 2009) showed that rates of propagation of retreating knickpoints depend on water discharge and substrate lithology. Paola et al. (1992) demonstrate that the equilibrium time (Teq) for fluvial systems to attain their graded profiles is influenced by the basin length (L) and the sediment-transport coefficient (v), which is determined by discharge, substrate lithology and relief, as expressed by the equation Teq = L^2/v. This suggests that higher water discharge should result in shorter equilibrium time (cf. Thorne, 1994), so that the recorded fluvial incision associated with high water discharge would be closer to the equilibrium profile. Blum et al. (2013) argue that for most fluvial systems Teq is within Milankovitch time scales, and that most rivers are not usually in equilibrium within their backwater lengths (Muto and Swenson, 2005). This view thus implies that for most of the late-Quaternary valley fills studied here, which formed in response to high-frequency sea-level change (Miller et al., 2005; Blum and Hattier-Womack, 2009; Blum et al., 2013), the equilibrium profile was not reached at lowstand (Strong and Paola, 2008). Under this assumption, the amount of valley incision recorded as valley-fill thickness must have been influenced by water discharge to varying degrees. Furthermore, water discharge and drainage-basin area correlate to maximum bankfull depths, which partly account for the depth of incision (Fielding and Crane, 1987; Bridge and Mackey, 1993; Shanley, 2004; Gibling, 2006; Fielding

et al., 2006; Syvitski and Milliman, 2007; Blum et al., 2013). Additionally, river lateral migration rates are strongly dependent on water discharge and sediment yield (Hooke, 1979, 1980; Nanson and Hickin, 1983; Lawler et al., 1999; Richard et al., 2005), implying that drainage-basin area should play a significant role in controlling incised-valley-fill width and cross-sectional area.
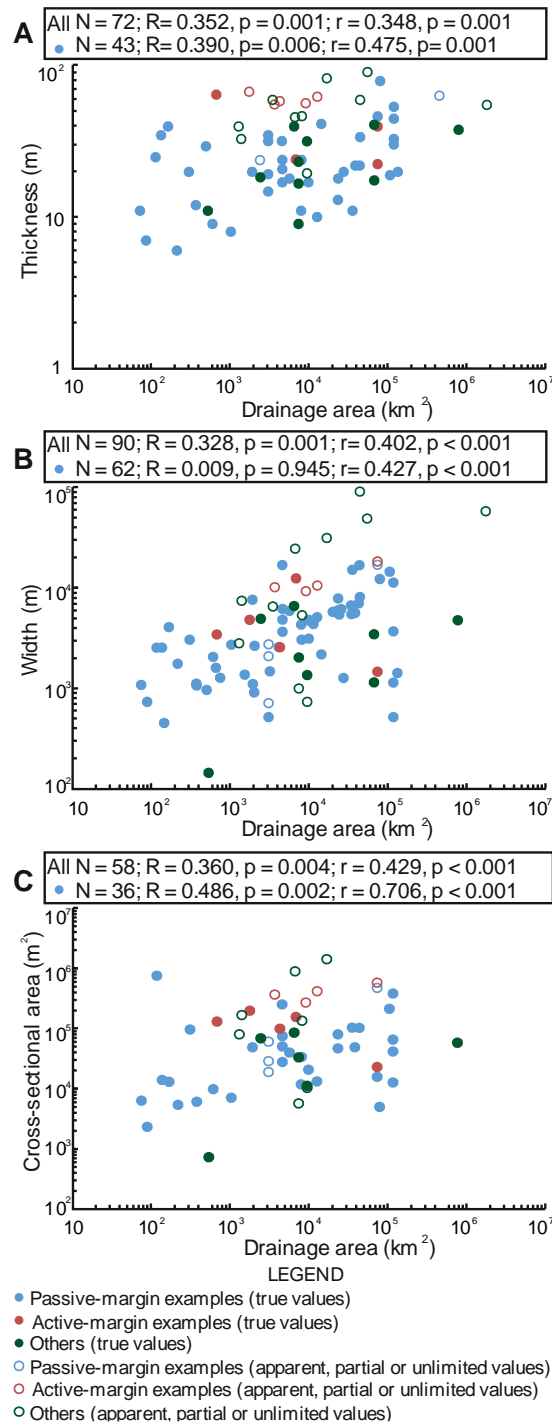

Fig. 12. Plots of: (A) incised-valley-fill thickness; (B) width; and (C) cross-sectional area versus drainage-basin area. For each pair of variables, the correlation coefficients of determination and p-values are reported in respective boxes. 'N' denotes the number of readings, 'R' denotes Pearson's R, and 'r' denotes Spearman's rho.

LGM catchment vegetation

Observations

Valley fills associated with catchments that are inferred to have mainly been covered by forests are, on average, considerably thinner than those with catchments covered by deserts or grasslands/woodlands (mean T = 23.74 m, 35.05 m, 34.15 m; one-way ANOVA: $F_{(2, 127)} = 3.59$, p-value = 0.03) (Fig. 13A); mean valley-fill width and cross-sectional area do not vary significantly over these three catchment vegetation types (one-way ANOVA: $F_{(2, 147)} = 3.86$, p-value =0.134 for W; $F_{(2, 93)} = 0.25$, p-value = 0.779 for A) (Fig. 13B and C). The thickness of valley fills with catchments covered mainly by tropical/subtropical vegetation types is on average significantly smaller than that with catchments covered by temperate or polar/subpolar vegetation (one-way ANOVA: $F_{(2, 127)} = 4.09$, p-value = 0.019, mean value = 24.33 m, 34.38 m, 36.13 m) (Fig. 13D). The means for valley-fill width and cross-sectional area are in agreement with this relationship (one-way ANOVA: $F_{(2, 147)} = 7.39$, p-value =0.001 for W; $F_{(2, 93)} = 3.93$, p-value = 0.023 for A) (Fig. 13E and F).
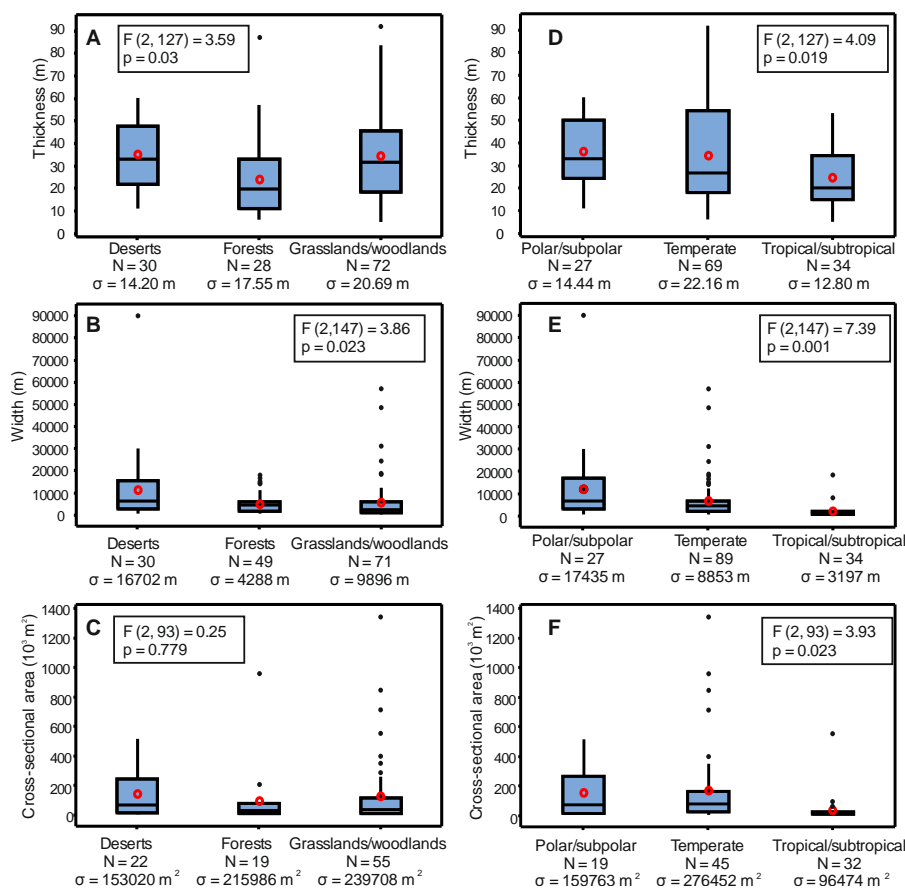
Fig. 13. Box plots of: (A) incised-valley-fill thickness; (B) width and (C) cross-sectional area distributions for different LGM catchment vegetation types ('forest', 'grassland or woodland', 'desert').Box plots of: (D) incised-valley-fill thickness; (E) width and (F) cross-sectional area distributions for different LGM catchment vegetation types ('tropical or subtropical', 'temperate', 'polar or subpolar'). For each boxplot, boxes represent interquartile ranges, red open circles represent mean values, horizontal bars within the boxes represent median values, and black dots represent outliers (values that are more than 1.5 times the interquartile range). 'N' denotes the number of readings. 'σ' denotes the standard deviation. The results of one-way ANOVA (F-value, p-value) are reported in respective boxes. The content bracketed in F-value are degrees of freedom between and within groups respectively.

Interpretations

Empirical analyses of modern river systems together with computer simulations (e.g., Vandenberghe, 2003; Latrubesse et al., 2011; Wohl et al., 2012) show that vegetation cover can influence the discharge of sediments and water by modulating evapotranspiration and runoff characteristics on the land surface, which in turn determine the degree and rates of fluvial incision and river migration (Hickin and Nanson, 1975, 1984; Blum and Törnqvist, 2000; Cecil et al., 2003; Blum et al., 2013). Drainage basins dominantly covered by tropical or subtropical vegetation types tend to have much more well-developed deep rooting systems and higher density of vegetation cover compared with their counterparts covered by other vegetation patterns; this typically causes stronger evapotranspiration and/or rainfall interception, resulting in stronger buffering of the surface runoff in the catchments and leading to decreased water discharge and decreased sediment supply to fluvial systems (Millar, 2000; Huisink, 2000; Huisink et al., 2002; Vandenberghe, 2003; Blum and Törnqvist, 2000; Blum et al., 2013), which in turn attenuates rates of fluvial incision and lateral migration. Our observations (Fig. 13D-F) might reflect these factors, and reveal that the inferred dominant vegetation type in the catchments of incised-valley fills during the LGM could have exerted a control on valley-fill thickness, width and cross-sectional area. However, these results only offer partial insight into the role of vegetation as a control on the geometry of incised-valley fills, given that the type and density of vegetation cover changed over the period of incised-valley formation and infill, especially at the apex of the coastal prism where the valleys experienced the longest sculpting by fluvial and marine processes (Mattheus and Rodriguez, 2011).

Latitude

Observations

Based on the global isotherms derived from atmospheric general circulation model reconstructions (Crowley and North 1991; Broecker 1995), inferred vegetation types (Adams and Faure, 1997; Ray and Adams, 2011), and other palaeotemperature estimates derived from sedimentological and zoological data (Adams and Faure, 1997; Ray and Adams, 2011), for the LGM, tropical zones are constrained to have been positioned between the Equator and 22° latitude, temperate zones to have lied between 22° to 50° latitude, and polar zones largely covered by ice sheets or polar and alpine deserts to have occurred above 50° latitude in both the northern and southern hemispheres. Based on the location where the incised-valley fills were measured, the LGC examples were classified in terms of these latitudinal belts. No significant difference is identified for means in valley-fill thickness and cross-sectional area across these latitudinal belts (one-way ANOVA: $F_{(2, 111)} = 0.15$, p-value=0.862 for T; $F_{(2, 85)} = 0.29$, p-value= 0.747 for A) (Fig. 14A and C). Incised-valley fills developed in the 22° to 50° latitudinal belt tend to be wider on average than those at lower latitudes (one-way ANOVA: $F_{(2, 129)} = 3.39$, p-value=0.037, mean = 6496.3 versus 4314.6 m) (Fig. 14B), even though incised valleys developed at latitudes from 0° to 22° are associated with drainage basins that are on average larger than their counterparts in the 22° to 50° range (2-sample t-test: t-value = 3.84, p-value = 0.001, df = 25) (Fig. 14D). For valley-fills developed between 0° and 22° latitude, valley-fill thickness tend to increase with latitude (r = 0.421, p-value = 0.040); no correlation is seen instead between valley-fill width or cross-sectional area and latitude (r(W) = 0.107, p-value = 0.626; r(A) = 0.252, p-value = 0.406) (Fig. 14E-G). The correlation between drainage-basin area and latitude is consistent with that for valley-fill thickness (r = 0.617, p-value = 0.004) (Fig. 14H). For valley-fills developed between 22° and 50° latitude, valley-fill thickness, width and cross-sectional area show weak or modest positive correlation with latitude

(r(T) = 0.204, p-value = 0.058; r(W) = 0.417, p-value < 0.001; r(A) = 0.416, p-value < 0.001) (Fig. 14E-G).
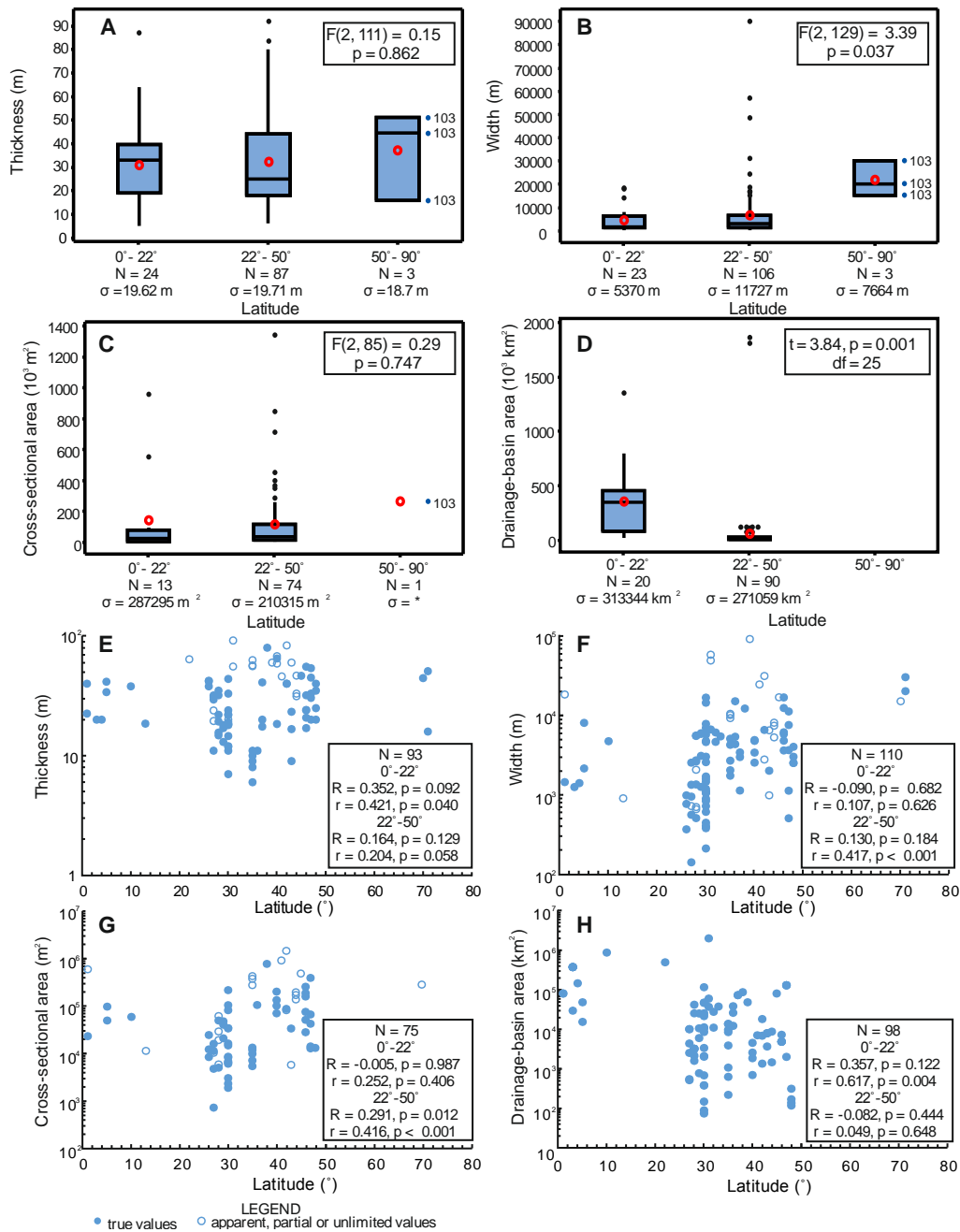
Fig. 14. Box plots of: (A) incised-valley-fill thickness; (B) width; (C) cross-sectional area; and (D) drainage-basin size distributions for different latitudinal belts. For each boxplot, boxes represent interquartile ranges, red open circles represent mean values, horizontal bars within the boxes represent median values, and black dots represent outliers (values that are more than 1.5 times the interquartile range). 'N' denotes the number of readings. 'σ' denotes the standard deviation. The results of one-way ANOVA (F-value, p-value) are reported in respective boxes. The content bracketed in F-value are degrees of freedom between and within groups respectively. Plots of: (E) incised-valley-fill thickness; (F) width; (G) cross-sectional area and (H) drainage-basin size versus latitude. For each pair of variables, the correlation coefficients of determination and p-values are reported in respective boxes. 'N' denotes the number of readings, 'R' denotes Pearson's R, and 'r' denotes Spearman's rho.

Interpretations

Through direct climatic forcing (e.g., temperature and peak precipitation), climate-derived forcing (e.g., presence of permafrost) and partially climate-dependent forcing (e.g., vegetation type), climate acts to influence the behaviour of fluvial systems (Blum and Törnqvist, 2000; Bogaart et al., 2003a, b; Vandenberghe, 2003). Compared with temperate zones, the tropical zones are typically characterized by more intense rainfalls and stronger weathering, which could have resulted in larger rates of delivery of water and sediment, enhancing rates of fluvial incision and river migration (Stallard et al., 1983; Milliman, 1995; Gupta, 2007; Goldsmith et al., 2008; Lloret, et al., 2011; Wohl et al., 2012). However, the distributions of incised-valley-fill dimensions for tropical zones and temperate zones (Fig. 14A-C) do not support this assumption. This might be due to the interplay of multiple climate-driven factors such as vegetation and precipitation, which have counteracting effects on water discharge and sediment supply and flux. Polar zones are dominated by ice caps or polar and alpine deserts: here, the size of fluvial catchments is limited as a result, but paraglacial and periglacial processes operate. Three of the studied incised-valley fills are located on the Alaskan Chukchi shelf (case study 103 in Table 1; Hill et al., 2007; Hill and Driscoll, 2008; Stockmaster, 2017), which, at the LGM, was a non-glaciated polar desert (Adams and Faure, 1997; Dyke, 2004; Ray and Adams, 2011). The large scale of these valley fills (Fig. 14A-C) might be attributed to enhanced fluvial incision and lateral migration (Kasse, 1997; Bogaart et al., 2003c; Vandenberghe, 2003), possibly due to periodic meltwater and sediment discharge from the Cordilleran Ice Sheet (Dyke, 2004) and in periglacial rivers (Woo and Winter, 1993; Vandenberghe, 2003), and to the occurrence of permafrost through its role in increasing surface runoff by lowering soil permeability (Church, 1983; Woo, 1986; Vandenberghe, 2003). Our observations (Fig.14A-C, E-G) indicate that during the LGM regional variations in incised-valley geometry might have been controlled by climate, in some contexts.

Substratum

Observations

The studied incised-valley fills were classified as either completely hosted in substrates made of unconsolidated sediments ('sedimentary cover'), or in substrates that are partly lithified or that might include basement rocks ('bedrock and sedimentary cover'). Incised-valley fills that are partially hosted in bedrock and sedimentary cover are thicker and wider on average than those hosted in sedimentary cover only (mean thickness = 40.0 m, 30.5 m; mean width = 11,822 m, 4,628 m), with the latter class varying from 15 m to 100 m in thickness and 500 m to 100,000 m in width (Fig. 15A-C). Mean valley-fill thickness and width are significantly different between these two populations (2-sample t-test: t-value = 2.24, p-value = 0.030, df = 43 for T and t-value = 2.31, p-value = 0.028, df = 33 for W) (Fig. 15B and C).

Interpretations

Substrate types play a significant role on fluvial incision rates (Van Heijst and Postma, 2001; Loget and Van Den Driessche, 2009; Gibling, 2006; Blum et al., 2013) and on the degree to which incision can progress to a graded profile in response to base-level lowering (Paola et al., 1992). Van Heijst and Postma (2001) and Loget and Van Den Driessche (2009) show that knickpoint-migration rates in alluvial settings are significantly larger than those in bedrock settings, corresponding to 1 to 20 m/yr and 0.001 to 0.1 m/yr, respectively. This would imply that valleys that are hosted in sedimentary cover are expected to be deeper than bedrock valley, any time before equilibrium is reached. In addition, the decreased erodibility of bedrock valley walls should result in narrower valley width. Results (Fig. 15) contrast with these expectations: this might be due to the fact that larger fluvial systems are more

likely to scour to the depth of lithified strata. In this sense, results would still not suggest that substrate lithology is a dominant control on valley-fill dimensions.
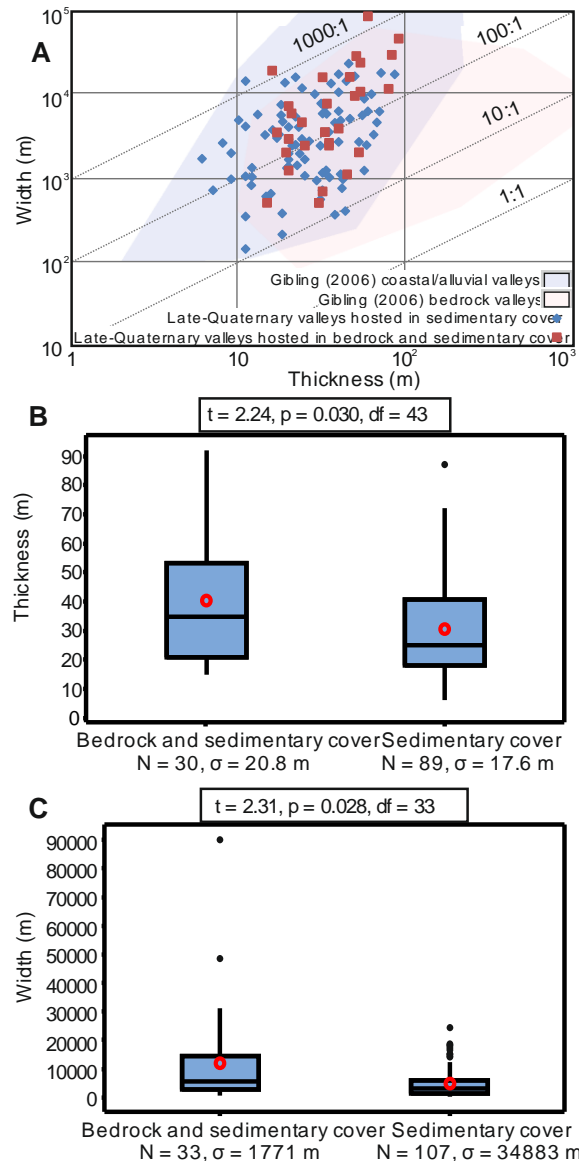
Fig. 15. (A) Scales of late-Quaternary valley fills hosted in bedrock and sedimentary cover and valley fills hosted in sedimentary cover versus incised-valley fills interpreted from ancient successions in the published literature. Ancient valley fills are adapted from Gibling (2006). Box plots of: (B) late-Quaternary incised-valley-fill thickness; and (C) width distributions for different substrate types. For each boxplot, boxes represent interquartile ranges, red open circles represent mean values, horizontal bars within the boxes represent median values, and black dots represent outliers (values that are more than 1.5 times the interquartile range). 'N' denotes the number of readings. 'σ' denotes the standard deviation. The results of 2-sample t-test (t-value, p-value and df) are reported in respective boxes. 'df' denotes the degrees of freedom between groups.

DISCUSSION

Controls on the dimensions of incised-valley systems and implications for sequence stratigraphic models

Previous workers have argued that the dimensions of near-shore incised valley systems are primarily a function of the magnitude and rate of relative base-level fall, basin physiography (gradients and convexity along the depositional profile and shelf-break depth), contributing drainage-basin size, climate, substrate characteristics and tectonics (Schumm, 1993; Talling, 1998; Posamentier and Allen, 1999; Blum and Törnqvist, 2000; Posamentier, 2001; Van Heijst and Postma, 2001; Gibling 2006; Strong and Paola, 2006, 2008; Loget and Van Den Driessche, 2009; Martin et al., 2011; Blum et al., 2013). Process-based studies argue that along continental margins, for a given relative sea-level fall, the physiography of the basin determines the largest vertical adjustment of a river system through valley incision (Talling, 1998; Posamentier and Allen, 1999; Posamentier, 2001; Törnqvist et al., 2006), whereas water discharge and substrate characteristics dominantly influence the degree to which, and rate at which, fluvial systems approach their equilibrium profile (Schumm et al., 1984; Paola et al., 1992; Van Heijst and Postma, 2001; Loget and Van Den Driessche, 2009; Loget and Van Den Driessche, 2009).

Our results (Fig. 5A-C) indicate that incised-valley systems and their fills developed along active continental margins are thicker and wider, on average, than those along passive continental margins, suggesting that the tectonic context of a continental margin plays a key role – at least indirectly – in determining the geometry of near-shore incised-valley systems. Through its effects on relative sea-level change, distinct characteristics of basin physiography, climate, water discharge and sediment delivery rates, the tectonic setting appears to control the magnitude of valley incision and widening (Posamentier and Allen, 1999; Jain and Tandon, 2003; Ishihara et al., 2011, 2012; Wohl et al., 2012; Tropeano et al., 2013; Vandenberghe, 2003; Ishihara and Sugai, 2017).

Mattheus et al. (2007), Mattheus and Rodriguez (2011) and Phillips (2011) claimed that valley-fill dimensions are primarily controlled by factors that act upstream, in particular by drainage-basin area, which serves as a proxy for water discharge and sediment yield. These authors report that valley-fill dimensions are less influenced by factors such as shelf-break depth, or coastal-plain and shelf gradients. Climate is also known to exert an important control on valley-fill dimensions, especially through modulation of temperature, peak precipitation, vegetation and permafrost in drainage-basin areas, which in turn dictates water discharge, rates of sediment supply and bank stability (Blum et al., 1994; Blum and Törnqvist, 2000; Vandenberghe, 2003; Bogaart et al., 2003a, b; Blum et al., 2013). The results (Fig. 12 and Fig. 13D-F) support the dominant role of drainage-basin characteristics in dictating incised-valley-fill dimensions, especially for passive continental margins, and highlight likely controls by the size and dominant vegetation type of catchment areas.

The physiography of the depositional profile over which incised valleys develop also plays a role in valley incision and widening (Summerfield, 1985; Talling, 1998; Posamentier and Allen, 1999; Posamentier, 2001; Blum and Törnqvist, 2000; Törnqvist et al., 2006; Blum et al., 2013). Along continental margins, valley incision tends to begin forming where a convex-up topography is exposed during relative sea-level fall (Summerfield, 1985; Talling, 1998; Blum and Törnqvist, 2000; Blum et al., 2013), which most commonly occurs at either the highstand coastline or at the shelf-slope break. Conceptual models (Talling, 1998; Posamentier and Allen, 1999; Posamentier, 2001; Törnqvist et al., 2006) highlight that when a sea-level fall causes exposure of the entire shelf, incised valleys will form across the whole shelf; on the contrary, when the shelf is only partially exposed by sea-level fall, incised valleys will only be limited to the region of the coastal prism. Additionally, it is embedded in sequence-

stratigraphic thinking (Posamentier and Allen, 1999) that the magnitude of incision associated with sequence boundaries is linked to the degree of exposure of the continental shelf. Contrary to this notion, it is observed that valley-fill dimensions for systems with shelf breaks that are shallower than 120 m tend to be smaller, on average, than systems on shelves that are deeper than 120 m (Fig. 6A-C). Nonetheless, the negative correlation between valley-fill thickness and shelf-break depth for cross-shelf valley fills hosted on shelves with shelf break shallower than 120 m (Fig. 7A) might indicate the expected causal link between magnitude of exposure, incision, and resulting valley-fill thickness, implying that the shelf-break depth plays a role in controlling valley-fill dimensions. Study on the relationships between shelf width, shelf gradient and cross-shelf valley dimensions (Fig. 8 and 10) might not indicate a causal link between these factors and cross-shelf valley dimensions. Rather, this might indicate shelf width, shelf gradient and cross-shelf valley dimensions co-vary in relation to a common control exerted by the size of drainage areas. The positive correlations between coastal-plain valley dimensions and shelf gradient (Fig. 10A and C) might be attributed to the fact that coastal-plain valley fills with steeper shelf gradient have a larger difference between shelf gradient and the original river equilibrium profile, which could lead to deeper fluvial incision for a given relative sea-level fall (Schumm and Brakenridge, 1987; Leckie, 1994; Posamentier and Allen, 1999). In addition, based on observations of present-day gradient profiles along passive margins and margins associated with foreland basins, Talling (1998) highlights that if the sea level remains above the shelf break, valley incision will be governed primarily by the geometry of the coastal prism and valley incision depth will tend to increase with the coastal-prism convexity. Our analysis of relationships between valley-fill dimensions and coastal-prism convexity (Fig. 11) challenges this widely held view and this might be due to the influence of overriding factors, or to the fact that the estimates of convexity for present-day costal prisms do not approximate the convexity of the coastal prisms established during the last interglacial.

In summary, the type of continental margin (active versus passive) appears to be a meaningful predictor of the geometry of incised-valley fills, presumably in relation to characteristics of basin physiography, climate, water discharge and sediment delivery (Fig. 16). In addition, our findings indicate that upstream controls (drainage-basin area) appear to be potentially more important than the characteristics of the receiving basin (e.g., coastal-prism convexity, shelf-break depth and substrate lithology) in determining rates and amounts of valley incision and widening, especially for passive continental margins.

Implications for source-to-sink studies and applied significance

The major components of source-to-sink systems – continent, shelf, slope and basin floor segments – are considered to be genetically related in analytical approaches that use mass-balance theory (Sømme et al., 2009a). Based on modern and late-Quaternary fluvial systems from different tectonic and climatic settings, recent work on source-to-sink systems (Anderson et al., 2004, 2016; Syvitski and Milliman, 2007; ; Sømme et al., 2009a,b; Blum et al., 2013; Xu et al., 2016; Sweet and Blum, 2016) has demonstrated scaling relationships between the scale of drainage-basin area, water discharge, river-driven sediment flux, channel-belt dimensions, and the corresponding scale of other distal components of sediment-dispersal systems (e.g. submarine canyons and basin-floor fans). Incised-valley systems play a key role in transferring sediments from hinterland regions to deep-marine environments, especially during lowstands (Posamentier and Allen, 1999; Blum and Törnqvist, 2000; Blum et al., 2013). The positive correlation between incised-valley-fill dimensions and contributing drainage-basin area (Fig. 12) documented here is important for source-to-sink analysis because it

provides a scaling relationship for incised-valley fills. The scale of incised-valley fills could be used to estimate the scales of their contributing drainage-basin areas and palaeodischarge, and also to predict scales of downdip coarse-grained lowstand deltas or basin-floor fans. Moreover, linking the scale of incised-valley fills to characteristics of catchments and shelves allows for the development of semi-quantitative guidelines that could be used to predict the size, location and timing of accumulation of potential hydrocarbon reservoirs. Incised-valley fills form important hydrocarbon reservoirs, typically characterized by coarser-grained fluvial deposits at their base and finer-grained estuarine and marine deposits at the top (Wright and Marriott, 1993; Shanley and McCabe, 1994; Zaitlin et al., 1994; Blum et al., 2013). However, as noted above, incised-valley-fill dimensions are influenced by a wide variety of geological controls and hence care should be taken for the exploration of incised-valley plays in different tectonic, physiographic and climatic settings. Notably, our results indicate that incised-valley fills along active continental margins can be thicker and wider than their counterparts along passive continental margins, highlighting the potential of the fills of incised valleys along active margins as exploration targets.
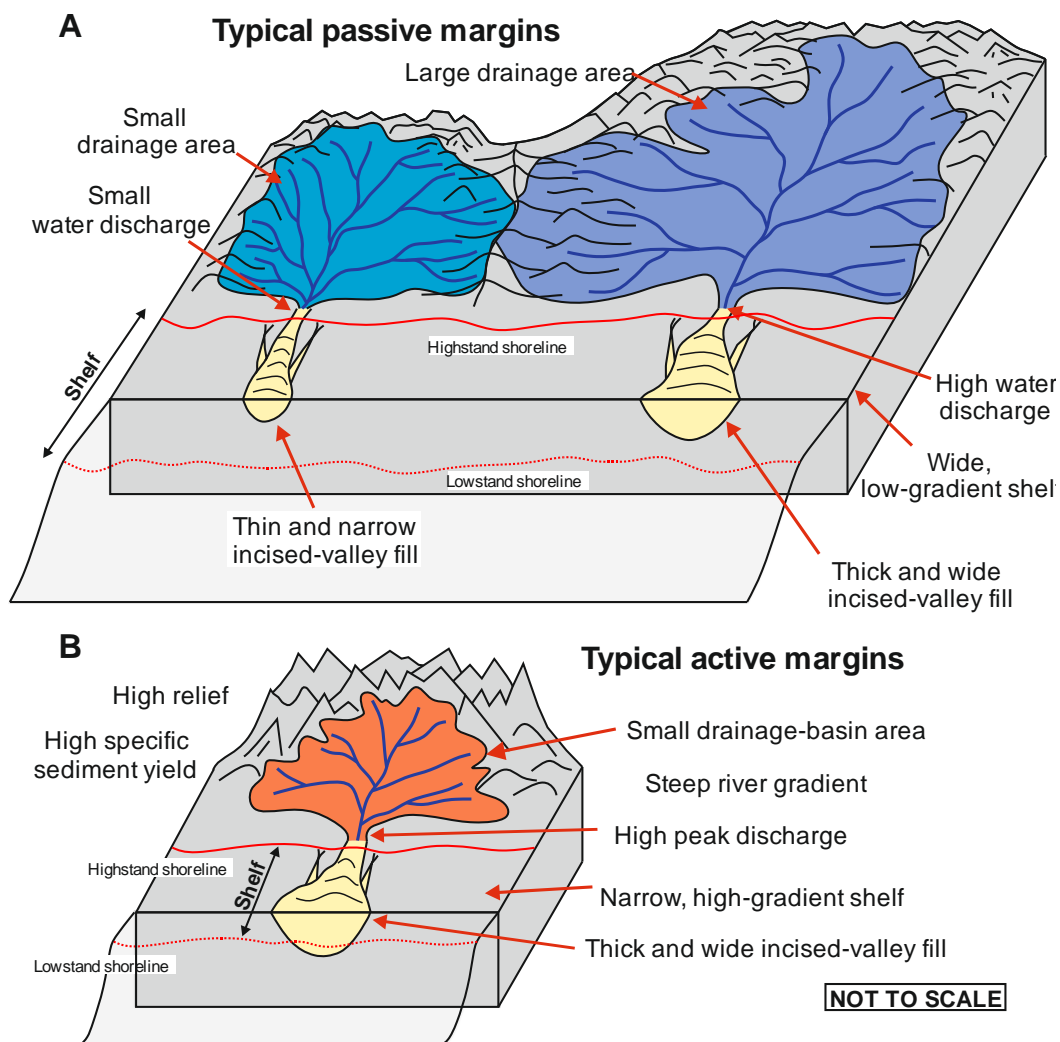

Fig. 16. Schematic diagrams of different incised-valley-fill dimensions corresponding to passive margins (A) and active margins (B). Along passive margins (A), the scale of incised-valley fills associated with large and small drainage-basin area respectively are compared.

CONCLUSIONS

A database-driven statistical analysis of 151 late-Quaternary incised-valley fills, which is the largest study of this type undertaken so far, has been performed with the aim to investigate controlling factors on the geometry of incised-valley fills.

Results of this analysis have been interpreted on the basis of some assumptions. The thickness of incised-valley fills is thought to be controlled by the degree of shelf or coastal plain incision – itself dictated, at any one location, by the vertical shifts in equilibrium profile driven by changes in base level, water discharge and sediment supply, and by the degree to which that profile is approximated in relation to knickpoint-retreat rates, together with potential truncation by ravinement processes. The width of the valley fills is determined by the rate of lateral migration of channel belts hosted within them, which again scales to water discharge and sediment supply, and by valley-wall erodibility. The main findings can be summarized as follows:

- Incised-valley fills developed along active margins are shown to be thicker and wider, on average, than those along passive margins. This indicates that the tectonic setting of continental margins appears to control the geometry of incised-valley fills, likely through its effects on relative sea-level change, and in relation to distinct characteristics of basin physiography, climate, water discharge and modes of sediment delivery.

- Valley-fill geometry is found to be positively correlated with the associated drainage-basin size, confirming the important role of drainage-basin area, a proxy of water discharge, in dictating valley-fill dimensions. This is especially true for incised-valley fills hosted on passive continental margins.

- Climate is also inferred to exert potential controls on valley-fill dimensions, especially through modulation of temperature, peak precipitation, vegetation and permafrost in drainage-basin areas, which in turn dictates water discharge, rates of sediment supply and valley-margin stability.

- Shelves with breaks currently deeper than 120 m contain thicker and wider incised-valley fills, on average, than shelves with breaks shallower than 120 m. This observation is at odds with the view that the magnitude of incision associated with sequence boundaries is linked to the degree of exposure of the continental shelf. This could be explained by the fact that the studied shelves with shelf breaks that are deeper than 120 m are primarily linked to larger drainage-basin areas, compared to those with shallower shelf breaks. Yet, negative correlation between valley-fill thickness and shelf-break depth for cross-shelf valley fills hosted on shelves whose margin is shallower than 120 m might indicate that shallow shelves record a causal link between magnitude of exposure, incision, and resulting valley-fill thickness.

- The lack of correlation between valley-fill thickness and present-day coastal-prism convexity challenges the idea that, especially if the sea level does not fall beyond the shelf break, the magnitude and location of valley incision should primarily be determined by the coastal-prism convexity. This discrepancy might alternatively be due to the influence of overriding factors (e.g., the size of drainage areas), or to the fact that present-day costal prisms do not approximate the form of coastal prisms established during the LI.

To some degree, these results challenge paradigms embedded in sequence stratigraphic thinking, and have significant implications for analysis and improved understanding of source-to-sink sediment route ways and for attempting semi-quantitative predictions of the occurrence and characteristics of hydrocarbon reservoirs. It is only through the analysis of very large composite datasets that describe the attributes of a large number of example systems that insight can be gained to demonstrably show the relative roles of many different controls which interact to determine the geometry of incised valley systems. This study accomplishes this via a novel database-driven approach.

ACKNOWLEDGEMENTS

REFERENCES CITED

Adams, J.M. and **Faure, H.** (1997) Preliminary vegetation maps of the world since the Last Glacial Maximum: an aid to archaeological understanding. J. Archaeol. Sci., **24**, 623–647.

Allen, G. P. and **Posamentier, H. W.** (1993) Sequence stratigraphy and facies model of an incised valley fill; the Gironde Estuary, France. J. Sed. Res., **63**, 378-391.

Alqahtani, F. A., Johnson, H. D., Jackson, C. A. L., and **Som, M. R. B.** (2015) Nature, origin and evolution of a Late Pleistocene incised valley-fill, Sunda Shelf, Southeast Asia. Sedimentology, **62**, 1198-1232.

Amorosi, A., Pacifico, A., Rossi, V., and Ruberti, D. (2012) Late Quaternary incision and deposition in an active volcanic setting: The Volturno valley fill, southern Italy. Sed. Geol., **282**, 307-320.

Amorosi, A., Rossi, V., Sarti, G., and Mattei, R. (2013) Coalescent valley fills from the late Quaternary record of Tuscany (Italy). Quatern. Int., **288**, 129-138.

Amorosi, A., Bracone, V., Campo, B., D'Amico, C., Rossi, V., and **Rosskopf, C. M.** (2016) A late Quaternary multiple paleovalley system from the Adriatic coastal plain (Biferno River, Southern Italy). Geomorphology, **254**, 146-159.

Anderson, J.B., Rodriguez, A., Abdulah, K.C., Fillon, R.H., Banfield, L.A., McKeown, H.A. and **Wellner, J.S.** (2004) Late Quaternary stratigraphic evolution of the northern Gulf of Mexico margin: a synthesis. In: Late Quaternary Stratigraphic Evolution of the Northern Gulf of Mexico Margin: A Synthesis (Eds J.B. Anderson and R.H. Fillon), SEPM Spec. Publ., **79**, 1–23.

Anderson, J.B., Wallace, D.J., Simms, A.R., Rodriguez, A.B., Weight, R.W., and **Taha, Z.P.** (2016) Recycling sediments between source and sink during a eustatic cycle: Systems of late Quaternary northwestern Gulf of Mexico Basin. Earth-Sci. Rev., **153**, 111–138.

Aquino da Silva, A. G., Stattegger, K., Schwarzer, K., and **Vital, H.** (2016) Seismic stratigraphy as indicator of late Pleistocene and Holocene sea level changes on the NE Brazilian continental shelf. J. S. Am. Earth Sci., **70**, 188-197.

Becker, J. J., Sandwell, D. T., Smith, W. H. F., Braud, J., Binder, B., Depner, J., Fabre, D., Factor, J., Ingalls, S., Kim, S. H., Ladner, R., Marks, K., Nelson, S., Pharaoh, A., Trimmer, R., Von Rosenberg, J., Wallace, G., and **Weatherall, P.** (2009) Global Bathymetry and Elevation Data at 30 Arc Seconds Resolution: SRTM30_PLUS. Mar. Geodesy, **32**, 355-371.

Bellotti, P., Caputo, C., Davoli, L., Evangelista, S., Garzanti, E., Pugliese, F., and **Valeri, P.** (2004) Morpho-sedimentary characteristics and Holocene evolution of the emergent part of the Ombrone River delta (southern Tuscany). Geomorphology, **61**, 71-90.

Benallack, K., Green, A. N., Humphries, M. S., Cooper, J. A. G., Dladla, N. N. and **Finch, J. M.** (2016) The stratigraphic evolution of a large back-barrier lagoon system with a non-migrating barrier. Mar. Geol., **379**, 64-77.

Blum, M.D. and **Price, D.M.** (1998) Quaternary alluvial plain construction in response to interacting glacio-eustatic and climatic controls, Texas Gulf Coastal Plain. In: Relative Role of Eustasy, Climate and Tectonism in Continental Rocks (Eds K.W. Shanley and P.J. McCabe), SEPM Spec. Publ., **59**, 31–48.

Blum, M.D. and **Törnqvist, T.E.** (2000) Fluvial responses to climate and sea-level change: A review and look forward. Sedimentology, **47**, 2–48.

Blum, M.D. and **Womack, J.H.** (2009) Climate change, sea-level change, and fluvial sediment supply to deepwater systems. In: External Controls on Deep Water Depositional Systems: Climate, Sea-Level, and Sediment Flux (Eds B. Kneller, O.J. Martinsen, and B. McCaffrey). SEPM Spec. Publ., **92**, 15–39.

Blum, M. D. and **Valastro, S., Jr.** (1994) Late Quaternary sedimentation, lower Colorado River, Gulf Coastal Plain of Texas. Geol. Soc. Am. Bull., **106**, 1002–1016.

Blum, M., Martin, J., Milliken, K. and **Garvin, M.** (2013) Paleovalley systems: Insights from Quaternary analogs and experiments. Earth-Sci. Rev., **116**, 128-169.

Bogaart, P. W., Balen, R. T. V., Kasse, C. and **Vandenberghe, J.** (2003) Process-based modelling of fluvial system response to rapid climate change—I: model formulation and generic applications. Quatern. Sci. Rev., **22**, 2077-2095.

Bogaart, P. W., Balen, R. T. V., Kasse, C. and **Vandenberghe, J.** (2003) Process-based modelling of fluvial system response to rapid climate change II. Application to the River Maas (The Netherlands) during the Last Glacial–Interglacial Transition. Quatern. Sci. Rev., **22**, 2097-2110.

Bogaart, P.W., Tucker, G.E. and **De Vries, J.J.** (2003) Channel network morphology and sediment dynamics under alternating periglacial and temperate regimes: a numerical simulation study. Geomorphology, **54**, 257-277.

Boyd, R., Dalrymple, R.W. and **Zaitlin, B.A.** (2006) Estuarine and incised-valley facies model. In: Facies Models Revisited (Eds H.W. Posamentier and R.G. Walker). SEPM Spec. Publ., **84**, 171–235.

Braudrick, C.A., Dietrich, W.E., Leverich, G.T. and **Sklar, L.S.** (2009) Experimental evidence for the conditions necessary to sustain meandering in coarse-bedded rivers. In: Proceedings of the National Academy of Sciences, **106**, 16936–16941.

Breda, A., Amorosi, A., Rossi, V., Fusco, F. and **Walsh, J. P.** (2016) Late-glacial to Holocene depositional architecture of the Ombrone palaeovalley system (Southern Tuscany, Italy): Sea-level, climate and local control in valley-fill variability. Sedimentology, **63**, 1124-1148.

Bridge, J.S. and **Mackey, S.D.** (1993) A theoretical study of fluvial sandstone body dimensions. In: Geological Modeling of Hydrocarbon Reservoirs and outcrop analogues (Eds S.S. Flint and I.D. Bryant). Int. Assoc. Sedimentol. Spec. Publ., **15**, 213–236.

Broecker, W. S. (1995) Cooling the tropics. Nature, **376**, 212-213.

Burgess, P. M., Steel, R. J. and **Granjeon, D.** (2008) Stratigraphic Forward Modeling of Basin-Margin Clinoform Systems: Implications for Controls on Topset and Shelf Width and Timing of Formation of Shelf-Edge Deltas. In: Recent Advances in Models of Siliciclastic Shallow-Marine Stratigraphy (Eds G. J. Hampson, R. J. Steel, P. M. Burgess and R. W. Dalrymple). SEPM Spec. Publ., **90**, 35-45.

Caputo, R., Bianca, M. and **D'Onofrio, R.** (2010) Ionian marine terraces of southern Italy: insights into the Quaternary tectonic evolution of the area. Tectonics, **29**, 24.

Catuneanu, O., Abreu, V., Bhattacharya, J.P., Blum, M.D., Dalrymple, R.W., Eriksson, P.G., Fielding, C.R., Fisher,W.L., Galloway,W.E., Gibling, M.R., Giles, K.A., Holbrook, J.M., Jordan, R., Kendall, C.G., St, C., Macurda, B., Martinsen, O.J., Miall, A.D., Neal, J.E., Nummedal, D., Pomar, L., Posamentier, H.W., Pratt, B.R., Sarg, J.F., Shanley, K.W., Steel, R.J., Strasser, A., Tucker, M.E., Winker, C. (2009) Toward the standardization of sequence stratigraphy. Earth-Science Reviews, **92**, 1-33.

Cecil, C.B. (2003) The concept of autocyclic and allocyclic controls on sedimentation and stratigraphy, emphasizing the climatic variable. In: Climate Controls on Stratigraphy (Eds C.B. Cecil and N.T. Edgar). SEPM Spec. Publ., **77**, 13–20.

Chaumillon, E. and **Weber, N.** (2006) Spatial variability of modern incised valleys on the French Atlantic coast: comparison between the Charente (Pertuis d'Antioche) and the Lay-Sèvre (Pertuis Breton) incised-valleys. In: Incised Valleys in Time and Space (Eds R.W. Dalrymple, D.A. Leckie and R.W. Tillman). SEPM Spec. Publ., **85**, 57–85.

Church, M. (1983) Pattern of instability in a wandering gravel bed channel. In: Modern and Ancient Alluvial Systems (Eds J.D. Collinson and J. Lewin). Int. Assoc. Sedimentol. Spec. Publ., **6**, 169–180.

Cilumbriello, A., Tropeano M. and **Sabato, L.** (2008) The Quaternary terraced marine-deposits of the Metaponto area (Southern Italy) in a sequence stratigraphic perspective. In: Advances in Application of Sequence Stratigraphy in Italy (Eds A. Amorosi, B.U. Haq and L. Sabato). GeoActa Special Publication, **1**, 29–54.

Cilumbriello, A. et al. (2010) Sedimentology, stratigraphic architecture and preliminary hydrostratigraphy of the Metaponto coastal-plain subsurface (Southern Italy). In: Proceedings of the National Workshop *"Multidisciplinary approach for porous aquifer characterization"* (Eds R. Bersezio and M. Amanti): Memorie descrittive della Carta Geologica d'Italia, **XC**, 67–84.

Colman, S.M. and **Mixon, R.B.** (1988) The record of major Quaternary sea-level changes in a large coastal plain estuary, Chesapeake Bay, eastern United States. Palaeogeogr. Palaeoclimatol. Palaeoecol., **68**, 99-116.

Colman, S.M., Halka, J.P., HOBBS III, C.H., Mixon, R.B. and **Foster, D.S.** (1990) Ancient channels of the Susquehanna River beneath Chesapeake Bay and the Delmarva peninsula. Geol. Soc. Am. Bull., **102**, 1268-1279.

Colombera, L., Mountney, N. P., Hodgson, D. M. and **McCaffrey, W. D.** (2016) The Shallow-Marine Architecture Knowledge Store: A database for the characterization of shallow-marine and paralic depositional systems. Mar. Petrol. Geol., **75**, 83-99.

Cooper, J.A.G., Green, A.N. and **Wright, C.I.** (2012) Evolution of an incised valley coastal plain estuary under lowsediment supply: a "give-up" estuary. Sedimentology, **59**, 899–916.

Cooper, J. A. G., Green, A. N., Meireles, R. P., Klein, A. H. F., Souza, J. and **Toldo, E. E.** (2016) Sandy barrier overstepping and preservation linked to rapid sea level rise and geological setting. Marine Geology, **382**, 80-91.

Crockett, J. S., Nittrouer, C. A., Ogston, A. S., Naar, D. F. and **Donahue, B. T.** (2008) Morphology and filling of incised submarine valleys on the continental shelf near the mouth of the Fly River, Gulf of Papua. J. Geophys. Res., **113**, no. F1.

Crowley, T. J. and **North, G. R.** (1991) Palaeoclimatology. Oxford, Oxford University Press.

Crumeyrolle, P. and **Renaud, I.** (2003) Quaternary incised valleys and low stand deltas imaged with 3D seismic and 2D HR profiles, Mahakam delta, Indonesia. AAPG International Conference, Barcelona, Spain, Extended Abstracts, **8**.

Dalrymple, R.W., Zaitlin, B.A. and **Boyd, R.** (1992) Estuarine facies models: conceptual basis and stratigraphic implications. J. Sed. Petrol., **62**, 1130–1146.

Dalrymple, R.W., Leckie, D.A., Tillman, R.W., eds. (2006) Incised valleys in time and space. SEPM Spec. Publ., **85**.

Dalrymple, R.W., Boyd, R and Zaitlin, B. A. (1994) Preface. In: Incised valley systems: Origins and sedimentary sequences (Eds R. W. Dalrymple, R. Boyd and B.A. Zaitlin). SEPM Spec. Publ., **51**, iii.

Daniell, J. J. (2008) Development of a bathymetric grid for the Gulf of Papua and adjacent areas: A note describing its development. J. Geophys. Res., **113**, F1.

Dietrich, W.E. and **Whiting, P.** (1989) Boundary shear stress and sediment transport in river meanders of sand and gravel. In: River Meandering (Eds H. Ikeda and G. Parker). AGU Water Resources Monograph, **12**, 1–50.

Doglioni, C., Tropeano, M., Mongelli, F. and **Pieri, P.** (1996) Middle-late Pleistocene uplift of Puglia: an "anomaly" in the Apenninic foreland. Memorie della Società Geologica Italiana, **51**, 101–117.

Dyke, A.S. (2004) An outline of North American deglaciation with emphasis on central and northern Canada. In: Developments in Quaternary Sciences, 373–424.

Fairbanks, R.G. (1989) A 17,000-year glacio-eustatic sea level record: influence of glacial melting rates on the Younger Dryas event and deep-ocean circulation. Nature, **342**, 637–642.

Fielding, C.R. and **Crane, R.C.** (1987) An application of statistical modelling to the prediction of hydrocarbon recovery factors in fluvial reservoir sequences. In: Recent Developments in Fluvial Sedimentology (Eds F.G. Ethridge, R.M. Flores and M.D. Harvey). SEPM Spec. Publ., **39**, 321–327.

Fielding, C. R., Trueman, J. D. and **Alexander, J. (2006)** Holocene Depositional History of the Burdekin River Delta of Northeastern Australia: A Model for a Low-Accommodation, Highstand Delta. J. Sed. Res., **76**, 411-428.

Fisk, H.N. (1944) Geological investigation of the alluvial valley of the lower Mississippi River. Vicksburg, Mississippi, U.S. Army Corps of Engineers Mississippi River Commission, 78 p., 33 plates.

Flint, J.J. (1974) Stream gradient as a function of order, magnitude, and discharge. Water Resour. Res., **10**, 969–973.

Foyle, A.M. and **Oertel, G.F.** (1992) Seismic stratigraphy and coastal drainage patterns in the Quaternary section of the southern Delmarva Peninsula, Virginia, USA. Sed. Geol., **80**, 261-277.

Foyle, A.M. and **Oertel, G.F.** (1997) Transgressive systems tract development and incised-valley fills within a Quaternary estuary-shelf system: Virginia inner shelf, USA. Mar. Geol., **137**, 227-249.

Geehan, G. and **J. Underwood** (1993) The use of shale length distributions in geological modeling. In: The geological modeling of hydrocarbon reservoirs and outcrop analogues (Eds S. Flint and I.D. Bryant). Int. Assoc. Sedimentol. Spec. Publ., **15**, 205-212.

Gibling, M.R. (2006) Width and thickness of fluvial channel bodies and valley fills in the geological record: A literature compilation and classification. J. Sed. Res., **76**, 731–770.

Goldsmith, S.T., Carey, A.E., Lyons, W.B., Kao, S.J. and **Chen, J.** (2008) Geochemical fluxes from the ChoShui River during Typhoon Mindulle, July 2004. Geology, **36**, 483-486.

Gomes, M. P., Vital, H., Stattegger, K. and **Schwarzer, K.** (2016) Bedrock control on the Assu Incised Valley morphology and sedimentation in the Brazilian Equatorial Shelf. International Journal of Sediment Research, **31**, 181-193.

Gonzalez, R., Dias, J.M.A., Lobo, F. and **Mendes, I.** (2004) Sedimentological and paleoenvironmental characterisation of transgressive sediments on the Guadiana Shelf (Northern Gulf of Cadiz, SW Iberia). Quatern. Int., **120**, 133-144.

Green, A. and **Luke Garlick, G.** (2011) A sequence stratigraphic framework for a narrow, current-swept continental shelf: The Durban Bight, central KwaZulu-Natal, South Africa. J. Afr. Earth Sci., **60**, 303-314.

Green, A. N., Cooper, J. A. G., Wiles, E. A. and **De Lecea, A. M.** (2015) Seismic architecture, stratigraphy and evolution of a subtropical marine embayment: Maputo Bay, Mozambique. Mar. Geol., **369**, 300-309.

Green, A. N. (2009) Palaeo-drainage, incised valley fills and transgressive systems tract sedimentation of the northern KwaZulu-Natal continental shelf, South Africa, SW Indian Ocean. Mar. Geol., **263**, 46-63.

Gupta, S., Collier, J. S., Palmer-Felgate, A. and **Potter, G.** (2007) Catastrophic flooding origin of shelf valley systems in the English Channel. Nature, **448**, 342-345.

Harris, P. T., Macmillan-Lawler, M., Rupp, J. and **Baker, E. K.** (2014) Geomorphology of the oceans. Mar. Geol., **352**, 4-24.

Helland-Hansen, W. and **Martinsen, O.J.** (1996) Shoreline trajectories and sequences: description of variable depositional-dip scenarios. J. Sed. Res., **66**, 670-688.

Helland-Hansen, W., Steel, R.J. and **Somme, T.O.** (2012) Shelf genesis revisited. J. Sed. Res., **82**, 133–1148.

Hickin, E.J. and **Nanson, G.C.** (1975) The character of channel migration of the Beatton River, northeast British Columbia, Canada. Geol. Soc. Am. Bull., **86**, 487–494.

Hickin, E.J. and **Nanson, G.C.** (1984) Lateral migration rates of river bends. J. Hydraul. Eng., **110**, 1557– 1567.

Hill, J. C. and **Driscoll, N. W.** (2008) Paleodrainage on the Chukchi shelf reveals sea level history and meltwater discharge. Mar. Geol., **254**, 129-151.

Hill, J. C., Driscoll, N. W., Brigham-Grette, J., Donnelly, J. P., Gayes, P. T. and **Keigwin, L.** (2007) New evidence for high discharge to the Chukchi shelf since the Last Glacial Maximum. Quatern. Res., **68**, 271-279.

Holbrook, J. and **Schumm, S.A.** (1999) Geomorphic and sedimentary response of rivers to tectonic deformation: a brief review and critique of a tool for recognizing subtle epeirogenic deformation in modern and ancient settings. Tectonophysics, **305**, 287-306.

Holbrook, J., Scott, R. W. and **Oboh-Ikuenobe, F. E.** (2006) Base-Level Buffers and Buttresses: A Model for Upstream Versus Downstream Control on Fluvial Geometry and Architecture Within Sequences. J. Sed. Res., **76**, 162-174.

Hooke, J.M. (1979) An analysis of the processes of river bank erosion. J. Hydrol., **42**, 39– 62.

Hooke, J.M. (1980) Magnitude and distribution of rates of river bank erosion. Earth Surface Processes, **5**, 143–157.

Huisink, M., de Moor, J.J.W., Kasse, C. and **Virtanen, T.** (2002) Factors influencing periglacial morphology in the northern European Russian tundra and taiga. Earth Surf. Proc. Land., **27**, 1223–1235.

Huisink, M. (2000) Changing river styles in response to Weichselian climate changes in the Vecht valley, eastern Netherlands. Sed. Geol., **133**, 115–134.

Ishihara, T. and **Sugai, T.** (2017) Eustatic and regional tectonic controls on late Pleistocene paleovalley morphology in the central Kanto Plain, Japan. Quatern. Int., **456**, 69-84.

Ishihara, T., Sugai, T. and **Hachinohe, S.** (2012) Fluvial response to sea-level changes since the latest Pleistocene in the near-coastal lowland, central Kanto Plain, Japan. Geomorphology, **147-148**, 49-60.

Ishihara, T., Sugai, T. and **Hachinohe, S.** (2011) Buried surfaces during the Last Glacial Age in the middle and upper part of the Arakawa Lowland and the Menuma Lowland, Central Japan. The Quatern. Res. (Japan), **50**, 113–128.

Jain, M. and **Tandon, S. K.** (2003) Fluvial response to Late Quaternary climate changes, western India. Quatern. Sci. Rev., **22**, 2223-2235.

Joeckel, R.M. (1999) Tectonic Uplift and Climate Change. Bulletin of the American Meteorological Society, **80**, 936.

Karisiddaiah, S.M., Veerayya, M. and **Vora, K.H.** (2002) Seismic and sequence stratigraphy of the central western continental margin of India: late-Quaternary evolution. Mar. Geol., **192**, 335-353.

Kasse, C. (1997) Cold-climate aeolian sand-sheet formation in north-western Europe (c. 14–12.4 ka): a response to permafrost degradation and increased aridity. Permafrost Periglac. Process., **8,** 295–311.

Kolla, V., Posamentier, H.W. and **Eichenseer, H.** (1995) Stranded parasequences and the forced regressive wedge systems tract: deposition during base-level fall- discussion. Sed. Geol., **95**, 139-145.

Korus, J. T., Kvale, E. P., Eriksson, K. A. and **Joeckel, R. M.** (2008) Compound paleovalley fills in the Lower Pennsylvanian New River Formation, West Virginia, USA. Sed. Geol., **208**, 15-26.

Labaune, C., Tesson, M. and **Gensous, B.** (2005) Integration of High and Very High-resolution Seismic Reflection Profiles to Study Upper Quaternary Deposits of a Coastal Area in the Western Gulf of Lions, SW France. Mar. Geophys. Res., **26**, 109-122.

Labaune, C., Tesson, M., Gensous, B., Parize, O., Imbert, P. and **Delhaye-Prat, V.** (2010) Detailed architecture of a compound incised valley system and correlation with forced regressive wedges: Example of Late Quaternary Têt and Agly rivers, western Gulf of Lions, Mediterranean Sea, France. Sed. Geol., **223**, 360-379.

Lambeck, K. and **Chappell, J.** (2001) Sea level change through the last glacial cycle. Science, **292**, 679-86.

Coe, M.T., Latrubesse, E.M., Ferreira, M.E. and **Amsler, M.L.** (2011) The effects of deforestation and climate variability on the streamflow of the Araguaia River, Brazil. Biogeochemistry, **105**, 119-131.

Lawler, D.M., Grove, J.R., Couperthwaite, J.S. and **Leeks, G.J.L.** (1999) Downstream change in river bank erosion rates in the Swale–Ouse system, northern England. Hydrological processes, **13**, 977-992.

Leckie, D.A. (1994) Canterbury Plains, New Zealand--implications for sequence stratigraphic models. AAPG Bull., **78**, 1240-1256.

Lee, G. S., Cukur, D., Yoo, D. G., Bae, S. H. and **Kong, G. S.** (2017) Sequence stratigraphy and evolution history of the continental shelf of South Sea, Korea, since the Last Glacial Maximum (LGM). Quatern. Int., **459**, 17-28.

Legarreta, L., and **Uliana, M.A.** (1998) **Anatomy** of hinterland depositional sequences: Upper Cretaceous fluvial strata, Neuquen Basin, west-central Argentina, in Shanley, K.W., and McCabe, P.J., eds., Relative Role of Eustasy Climate and Tectonism in Continental Rocks. SEPM Spec. Publ., **59**, 83–92.

Lericolais, G., Berné, S. and **Féniès, H.** (2001) Seaward pinching out and internal stratigraphy of the Gironde incised valley on the shelf (Bay of Biscay). Mar. Geol., **175**, 183-197.

Li Congxian, Wang Ping, Sun Heping, Zhang Jianqiang, Fan Daidu and **Deng Bing** (2002) Late Quaternary incised-valley fill of the Yangtze delta (China): its stratigraphic framework and evolution. Sed. Geol., **152**, 133-158.

Li Congxian, Wang Ping, Fan Daidu and **Yang Shouye** (2006) Characteristics and formation of Late Quaternary incised-valley-fill sequences in sediment-rich deltas and estuaries: case studies from China. In: Incised Valleys in Time and Space (Eds R.W. Dalrymple, D.A. Leckie and R.W. Tillman). SEPM Spec. Publ., **85**, 141-160.

Lloret, E., Dessert, C., Gaillardet, J., Albéric, P., Crispi, O., Chaduteau, C. and **Benedetti, M.F.** (2011) Comparison of dissolved inorganic and organic carbon yields and fluxes in the watersheds of tropical volcanic islands, examples from Guadeloupe (French West Indies). Chem. Geol., **280**, 65-78.

Lobo, F.J., Hernández-Molina, F.J., Somoza, L. and **del Río, V.D.** (2001) The sedimentary record of the post-glacial transgression on the Gulf of Cadiz continental shelf (Southwest Spain). Mar. Geol., **178**, 171-195.

Lobo, F.J., García, M., Luján, M., Mendes, I., Reguera, M.I. and **Van Rooij, D.** (2018) Morphology of the last subaerial unconformity on a shelf: insights into transgressive ravinement and incised valley occurrence in the Gulf of Cádiz. Geo-Mar. Lett., **38**, 33-45.

Lockhart, D.A., Lang, S.C. and **Allen, G.P.** (1996) Stratal Architecture and Seismic Stratigraphy of Late Quaternary Bedrock-Controlled Incised Valley Systems, Southern Moreton Bay, Australia. In: Proceedings, the International Symposium on Sequence Stratigraphy, S.E. Asia, May 1995.

Loget, N. and **Van Den Driessche, J.** (2009) Wave train model for knickpoint migration. Geomorphology, **106**, 376–382.

Mackey, S.D. and **Bridge, J.S.** (1995) Three-dimensional model of alluvial stratigraphy: theory and application. J. Sed. Res., **65**, 7-31.

Makinouchi, T., Mori, S., Danhara, T. and **Takemura, K.** (2006) Stratigraphic horizon and formational process of the First Gravel Formation (BG) in the Nohbi Plain. In: Recent Progress on the Understanding of So-called Chuseki-so: The Memoirs of the Geological Survey of Japan (Chishitsugaku Ronshu) (Eds Y. Inouchi et al.), **59**, 129-139.

Martin, J., Cantelli, A., Paola, C., Blum, M. and **Wolinsky, M.** (2011) Quantitative Modeling of the Evolution and Geometry of Incised Valleys. J. Sed. Res., **81**, 64-79.

Maselli, V. and **Trincardi, F.** (2013) Large-Scale Single Incised Valley from a Small Catchment Basin on the Western Adriatic Margin (central Mediterranean Sea). Global Planet. Change, **100**, 245–262.

Maselli, V., Trincardi, F., Asioli, A., Ceregato, A., Rizzetto, F. and **Taviani, M.** (2014) Delta growth and river valleys: the influence of climate and sea level changes on the South Adriatic shelf (Mediterranean Sea). Quatern. Sci. Rev., **99**, 146-163.

Mattheus, C. R. and **Rodriguez, A. B.** (2011) Controls on late Quaternary incised-valley dimension along passive margins evaluated using empirical data. Sedimentology, **58**, 1113-1137.

Mattheus, C. R., A. B. Rodriguez, D. L. Greene, A. R. Simms and **J. B. Anderson** (2007) Control of Upstream Variables on Incised-Valley Dimension. J. Sed. Res., **77**, 213–224.

Menier, D., Reynaud, J.Y., Proust, J.N., Guillocheau, F., Guennoc, P., Bonnet, S., Tessier, B. and **Goubert, E.** (2006) Basement control on shaping and infilling of valleys incised at the southern coast of Brittany, France. In: Incised Valleys in Time and Space (Eds R.W. Dalrymple, D.A. Leckie and R.W. Tillman). SEPM Spec. Publ., **85**, 37-55.

Miall, A.D. (2002) Architecture and sequence stratigraphy of Pleistocene fluvial systems in the Malay Basin, based on seismic time-slice analysis. AAPG Bull., **86**, 1201–1216.

Millar, R.G. (2000) Influence of bank vegetation on alluvial channel patterns. Water Resour. Res., **36**, 1109–1118.

Miller, K.G., Kominz, M.A., Browning, J.V., Wright, J.D., Mountain, G.S., Katz, M.E., Sugarman, P.J., Cramer, B.S., Christie-Blick and **N., Pekar, S.F.** (2005) The Phanerozoic record of global sea-level change. Science, **310**, 1293–1298.

Milli, S., D'Ambrogi, C., Bellotti, P., Calderoni, G., Carboni, M. G., Celant, A., Di Bella, L., Di Rita, F., Frezza, V., Magri, D., Pichezzi, R. M. and **Ricci, V.** (2013) The transition from wave-dominated estuary to wave-dominated delta: The Late Quaternary stratigraphic architecture of Tiber River deltaic succession (Italy). Sed. Geol., **284-285**, 159-180.

Milli, S., Mancini, M., Moscatelli, M., Stigliano, F., Marini, M., Cavinato, G. P. and **Mohrig, D.** (2016) From river to shelf, anatomy of a high-frequency depositional sequence: The Late Pleistocene to Holocene Tiber depositional sequence. Sedimentology, **63**, 1886-1928.

Milliman, J. D. and **Syvitski, J. P. M.** (1992) Geomorphic/tectonic control of sediment discharge to the oceans: The importance of small mountainous rivers. J. Geol., **100**, 525–544.

Milliman, J.D. (1995) Sediment discharge to the ocean from small mountainous rivers: the New Guinea example. Geo-Mar. Lett., **15**, 127-133.

Mitchum, R.M. (1985) Seismic stratigraphic expression of submarine fans. In: Seismic Stratigraphy II—An Integrated Approach (Eds O.R. Berg and D.G. Woolverton). AAPG Memoir, **39**, 116–136.

Morton, R.A. and **Suter, J.R.** (1996) Sequence stratigraphy of composition of late Quaternary shelf-margin deltas, northern Gulf of Mexico. AAPG Bull., **80**, 505-530.

Muto, T. and **Swenson, J.B.** (2005) Large-scale fluvial grade as a nonequilibrium state in linked depositional systems: Theory and experiment. J. Geophys. Res., **110**, F3.

Nanson, G.C. and **Hickin, E.J.** (1983) Channel migration and incision on the Beatton River. J. Hydraul. Eng., **109**, 327-337.

Nanson, G.C. and **Hickin, E.J.** (1986) A statistical analysis of bank erosion and channel migration in western Canada. Geol. Soc. Am. Bull., **97**, 497-504.

Ngueutchoua, G. and **Giresse, P.** (2010) Sand bodies and incised valleys within the Late Quaternary Sanaga–Nyong delta complex on the middle continental shelf of Cameroon. Mar. Petrol. Geol., **27**, 2173-2188.

Nordfjord, S., Goff, J. A., Austin, J. A. and **Sommerfield, C. K.** (2005) Seismic geomorphology of buried channel systems on the New Jersey outer shelf: assessing past environmental conditions. Mar. Geol., **214**, 339-364.

Nordfjord, S., Goff, J. A., Austin, J. A. and **Gulick, S. P. S.** (2006) Seismic Facies of Incised-Valley Fills, New Jersey Continental Shelf: Implications for Erosion and Preservation Processes Acting During Latest Pleistocene-Holocene Transgression. J. Sed. Res., **76**, 1284-1303.

Oertel, G.F. and **Foyle, A.M.** (1995) Drainage displacement by sea-level fluctuation at the outer margin of the Chesapeake Seaway. J. Coastal Res., **11**, 583-604.

Olariu, C. and **Steel, R. J.** (2009) Influence of point-source sediment-supply on modern shelf-slope morphology: implications for interpretation of ancient shelf margins. Basin Res., **21**, 484-501.

Paola, C., Heller, P.L. and **Angevine, C.L.** (1992) The large-scale dynamics of grain-size variation in alluvial basins, 1: Theory. Basin Res., **4**, 73-90.

Patacca, E. and **Scandone, P.** (2001) Late thrust propagation and sedimentary response in the thrust belt-foredeep system of the Southern Apennines (Pliocene–Pleistocene), In: Anatomy of an Orogen: Kluwer Academic Publication (Eds G.B. Vai and I.P. Martini), 401–440.

Payenberg, T.H., Boyd, R., Beaudoin, J., Ruming, K., Davies, S., Roberts, J. and **Lang, S.C.** (2006) The filling of an incised valley by shelf dunes—an example from Hervey Bay, east coast of Australia In: Incised Valleys in Time and Space (Eds R.W. Dalrymple, D.A. Leckie and R.W. Tillman). SEPM Spec. Publ., **85**, 87-98.

Peakall, J., Ashworth, P.J. and **Best, J.L.** (2007) Meander-bend evolution, alluvial architecture, and the role of cohesion in sinuous river channels: a flume study. J. Sed. Res., **77**, 197–212.

Peltier, W.R. and **Fairbanks, R.G.** (2006) Global glacial ice volume and Last Glacial Maximum Duration from an extended Barbados sea level record. Quatern. Sci. Rev., **25**, 3322–3337.

Phillips, J. D. (2011) Drainage area and incised valley fills in Texas rivers: A potential explanation. Sed. Geol., **242**, 65-70.

Posamentier, H.W., Allen, G.P., James, D.P. and **Tesson, M.** (1992) Forced regressions in a sequence stratigraphic framework: concepts, examples and exploration significance. AAPG Bull., **76**, 1687-1709.

Posamentier, H.W. and **Vail, P.R.** (1988) Eustatic controls on clastic deposition II — sequence and systems tract models. In: Sea Level Changes: An Integrated Approach (Eds C.K. Wilgus, B.S. Hastings, C.G.St.C. Kendall, H.W. Posamentier, C.A. Ross, J.C. Van Wagoner). SEPM Spec. Publ., **42**, 125–154.

Posamentier, H.W. (2001) Lowstand alluvial bypass systems: incised vs. unincised. AAPG Bull., **85**, 1771–1793.

Proust, J.N., Renault, M., Guennoc, P. and **Thinon, I.** (2010) Sedimentary architecture of the Loire River drowned valleys of the French Atlantic shelf. Bulletin de la Société géologique de France, **181**, 129-149.

Ray, N. and **Adams, J.** (2001) A GIS-based vegetation map of the world at the last glacial maximum (25,000-15,000 BP). Internet archaeology, 11.

Reijenstein, H. M., Posamentier, H. W. and **Bhattacharya, J. P.** (2011) Seismic geomorphology and high-resolution seismic stratigraphy of inner-shelf fluvial, estuarine, deltaic, and marine sequences, Gulf of Thailand. AAPG Bull., **95**, 1959-1990.

Richard, G. A., Julien, P. Y. and **Baird, D. C.** (2005) Statistical analysis of lateral migration of the Rio Grande, New Mexico. Geomorphology, **71**, 139-155.

Roberts, H.H. and **Sydow, J.** (2003) Late Quaternary stratigraphy and sedimentology of the offshore Mahakam delta, east Kalimantan (Indonesia). In: Tropical Deltas of Southeast Asia—Sedimentology, Stratigraphy, and

Petroleum Geology (Eds F.H. Sidi, D. Nummedal, P. Imbert, H. Darman and H.W. Posamentier). SEPM Spec. Publ., **76**, 125-145.

Rodriguez, A.B., Anderson, J.B. and **Simms, A.R.** (2005) Terrace inundation as an autocyclic mechanism for parasequence formation: Galveston Estuary, Texas, USA. J. Sed. Res., **75**, 608-620.

Rossi, V., Amorosi, A., Sarti, G., Mariotti, S. and **Marzo, M.** (2017) Late Quaternary multiple incised valley systems: An unusually well-preserved stratigraphic record of two interglacial valley-fill successions from the Arno Plain (northern Tuscany, Italy). Sedimentology, **64**, 1901-1928.

Roy, P.S. (1984) New South Wales Estuaries: their origin and evolution. In: Coastal Geomorphology in Australia (Ed Thom, B.G.). Academic Press, Sydney, Australia, 99–121.

Ruddiman, W.F. (2013) Tectonic uplift and climate change. Springer Science & Business Media.

Schneider, C.A., Rasband, W.S. and **Eliceiri, K.W.** (2012) NIH Image to ImageJ: 25 years of image analysis. Nature methods, **9**, 671.

Schumm, S.A. and **Brackenridge, S.A.** (1987) River response. In: North America and Adjacent Oceans during the Last Deglaciation (Eds W.F. Ruddiman and H.E. Wright, Jr), Geol. Soc. Am., The Geology of North America, **K-3**, 221–240.

Schumm, S.A., Harvey, M.D. and **Watson, C.C.** (1984) Incised Channels: Morphology, Dynamics and Control. Water Resources Publication, Chelsea, MI, 200 pp.

Schumm, S. A. (1993) River response to base-level change: Implications for sequence stratigraphy. J. Geol., **101**, 279–294.

Shanley, K.W. and **McCabe, P.J.** (1994) Perspectives on the sequence stratigraphy of continental strata: report of a working group at the 1991 NUNA conference of high resolution sequence stratigraphy. AAPG Bull., **78**, 544–568.

Shanley, K.W. (2004) Fluvial reservoir description for a giant, low-permeability gas field: Jonah Field, Green River Basin, Wyoming, U.S.A.

Sheets, B.A., Hickson, T.A. and **Paola, C.** (2002) Assembling the stratigraphic record: depositional patterns and time-scales in an experimental alluvial basin. Basin Res., **14**, 287–301.

Shideler, G.L., Ludwick, J.C., Oertel, G.F. and **Finkelstein, K.** (1984) Quaternary stratigraphic evolution of the southern Delmarva Peninsula coastal zone, Cape Charles, Virginia. Geol. Soc. Am. Bull., **95**, 489-502.

Simms, A.R., Anderson, J.B., Milliken, K.T., Taha, Z.P. and **Wellner, J.S.** (2007a) Geomorphology and age of the OIS2 (last lowstand) sequence boundary on the northwestern Gulf of Mexico continental shelf. In: Seismic Geomorphology: Applications to Hydrocarbon Exploration and Production (Eds R.J. Davies, H.W. Posamentier, L.J. Wood and J.A. Cartwright), Geol. Soc. London Spec. Publ., **277**, 29–46.

Simms, A.R., Lambeck, K., Purcell, A., Anderson, J.B. and **Rodriguez, A.B.** (2007b) Sea-level history of the Gulf of Mexico since the Last Glacial Maximum with implications for the melting history of the Laurentide Ice Sheet. Quatern. Sci. Rev., **26**, 920-940.

Sømme, T.O., Helland-Hansen, W., Martinsen, O.J. and **Thurmond, J.B.** (2009a) Relationships between morphological and sedimentological parameters in source-to-sink systems: A basis for predicting semi-quantitative characteristics in subsurface systems. Basin Res., **21**, 361–387.

Sømme, T.O., Martinsen, O.J. and **Thurmond, J.B.** (2009b) Reconstructing morphological and depositional characteristics in subsurface sedimentary systems: An example from the Maastrichtian-Danian Ormen Lange system, Møre Basin, Norwegian Sea. AAPG Bull., **93**, 1347–1377.

Stallard, R.F. and **Edmond, J.M.** (1983) Geochemistry of the Amazon: 2. The influence of geology and weathering environment on the dissolved load. J. Geophys. Res.: Oceans, 88(C14), 9671-9688.

Stockmaster, B.A. (2017) Paleodrainage insights into the fluvial and glacial history of the western Chukchi margin, Arctic Alaska [Ph.D. thesis]. Coastal Carolina University, 45-73 pp.

Strong, N. and **Paola, C.** (2006) Fluvial landscapes and stratigraphy in a flume. Sed. Rec., **4**, 4–8.

Strong, N. and **Paola, C.** (2008) Valleys that never were: time surfaces versus stratigraphic surfaces. J. Sed. Res., **78**, 579–593.

Sugai, T. and **Sugiyama, Y.** (1998) Deep Seismic Reflection Survey of Concealed Active Structures in the Nobi Basin Dynamics and Subsidence History of the Nobi Plain, Central Japan. Geological Survey of Japan Interim Report EQ/98/1, 55-66 (in Japanese with English abstract).

Sugai, T. and **Sugiyama, Y.** (1999) Basin Dynamics and Subsidence History of the Nobi Plain, Central Japan, Revealed by 600 M Deep Core Analysis and Deep Seismic Reflection Survey. Geological Survey of Japan Interim Report EQ/99/3, 77-87 (in Japanese with English abstract).

Summerfield, M.A. (1985) Plate tectonics and landscape development on the African continent. Tectonic Geomorphology, 27–51.

Sweet, M. L. and **Blum, M. D.** (2016) Connections Between Fluvial To Shallow Marine Environments and Submarine Canyons: Implications For Sediment Transfer To Deep Water. J. Sed. Res., **86**, 1147-1162.

Sydow, J.C. (1996) Holocene to Late Pleistocene Stratigraphy of the Mahakam Delta, Kalimantan, Indonesia [Ph.D. thesis]. Louisiana State University.

Syvitski, J.P.M. and **Milliman, J.D.** (2007) Geology, geography, and humans battle for dominance over the delivery of fluvial sediment to the coastal ocean. J. Geol., **115**, 1–19.

Talling, P.J. (1998) How and where to incised valleys form in sea level remains above the shelf edge? Geology, **26**, 87–90.

Tesson, M., Labaune, C., Gensous, B., Suc, J. P., Melinte-Dobrinescu, M., Parize, O., Imbert, P. and **Delhaye-Prat, V.** (2011) Quaternary "Compound" Incised Valley In A Microtidal Environment, Roussillon Continental Shelf, Western Gulf of Lions, France. J. Sed. Res., **81**, 708-729.

Tesson, M., Posamentier, H. and **Gensous, B.** (2015) Compound incised-valley characterization by high-resolution seismics in a wave-dominated setting: Example of the Aude and Orb rivers, Languedoc inner shelf, Gulf of Lion, France. Mar. Geol., **367**, 1-21.

Thomas, M.A. and **Anderson, J.B.** (1994) Sea-level controls on the facies architecture of the Trinity/Sabine incised-valley system, Texas continental shelf. In: Incised-Valley Systems: Origin and Sedimentary Sequences (Eds R.W. Dalrymple, R. Boyd and B.A. Zaitlin), SEPM Spec. Publ., **51**, 63–82.

Thorne, J. (1994) Constraints on riverine valley incision and the response to sea-level change based on fluid mechanics. In: Incised-Valley Systems: Origin and Sedimentary Sequences (Eds R.W. Dalrymple, R. Boyd and B.A. Zaitlin), SEPM Spec. Publ., **51**, 29–45.

Tjallingii, R., Stattegger, K., Wetzel, A. and **Van Phach, P.** (2010) Infilling and flooding of the Mekong River incised valley during deglacial sea-level rise. Quatern. Sci. Rev., **29**, 1432-1444.

Törnqvist, T. E., Wortman, S. R., Mateo, Z. R. P., Milne, G. A. and **Swenson, J. B.** (2006) Did the last sea level lowstand always lead to cross-shelf valley formation and source-to-sink sediment flux? J. Geophys. Res., **111**, F04002.

Tropeano, M., Cilumbriello, A., Sabato, L., Gallicchio, S., Grippa, A., Longhitano, S. G., Bianca, M., Gallipoli, M. R., Mucciarelli, M. and **Spilotro, G.** (2013) Surface and subsurface of the Metaponto Coastal Plain (Gulf of Taranto—southern Italy): Present-day- vs LGM-landscape. Geomorphology, **203**, 115-131.

Twichell, D. C., Cross, V. A. and **Peterson, C. D.** (2010) Partitioning of sediment on the shelf offshore of the Columbia River littoral cell. Mar. Geol., **273**, 11-31.

Van Heijst, M.W.I.M. and **Postma, G.** (2001) Fluvial response to sea-level changes: a quantitative analogue, experimental approach. Basin Res., **13**, 269-292.

Van Wagoner, J.C., Posamentier, H.W., Mitchum, R.M., Vail, P.R., Sarg, J.F., Loutit, T.S. and **Hardenbol, J.** (1988) An overview of sequence stratigraphy and key definitions. In: Sea-level Changes: An Integrated Approach (Eds C.K. Wilgus, B.S. Hastings, C.G.St.C. Kendall, H.W. Posamentier, C.A. Ross and J.C. Van Wagoner), SEPM Spec. Publ., **42**, 39–45.

Van Wagoner, J.C., Mitchum, R.M., Campion, K.m. and **Rahmanian, V.D.** (1990) Siliciclastic sequence stratigraphy in well logs, core, and outcrops: concepts for high-resolution correlation of time and facies. Am. Assoc. Petrol. Geol., Meth. Explor. Ser., **7**, 55.

Vandenberghe, J. (2003) Climate forcing of fluvial system development: an evolution of ideas. Quatern. Sci. Rev., **22**, 2053-2060.

Vis, G.J., Kasse, C. (2009) Late Quaternary valley fill succession of the Lower Tagus Valley, Portugal. Sed. Geol., **221**, 19–39.

Vis, G.-J., Kasse, C. and **Vandenberghe, J.** (2008) Late Pleistocene and Holocene palaeogeography of the Lower Tagus Valley (Portugal): effects of relative sea level, valley morphology and sediment supply. Quatern. Sci. Rev., **27**, 1682-1709.

Vital, H., Furtado, S.F.L. and **Gomes, M.P.** (2010) Response of the Apodi-Mossoró estuary-incised valley system (NE Brazil) to sea-level fluctuations. Brazilian journal of Oceanography, **58**, 13-24.

Weber, N., Chaumillon, E., Tesson, M. and **Garlan, T.** (2004) Architecture and morphology of the outer segment of a mixed tide and wave-dominated-incised valley, revealed by HR seismic reflection profiling: the paleo-Charente River, France. Mar. Geol., **207**, 17-38.

Wellner, R.W. and **Bartek, L.R.** (2003) The effect of sea level, climate, and shelf physiography on the development of incised-valley complexes: a modern example from the East China Sea. J. Sed. Res., **73**, 926-940.

Weschenfelder, J., Baitelli, R., Corrêa, I.C., Bortolin, E.C. and **dos Santos, C.B.** (2014) Quaternary incised valleys in southern Brazil coastal zone. J. S. Am. Earth Sci., **55**, 83-93.

Wilson, K., Berryman, K., Cochran, U. and **Little, T.** (2007) A Holocene incised valley infill sequence developed on a tectonically active coast: Pakarae River, New Zealand. Sed. Geol., **197**, 333-354.

Wohl, E. et al. (2012) The hydrology of the humid tropics. Nature Climate Change, **2**, 655-662.

Woo, M.K., Winter, T.C. (1993) The role of permafrost and seasonal frost in the hydrology of northern wetlands in North America. J. Hydrol., **141**, 5–31.

Woo, M.K. (1986) Permafrost hydrology in North America. Atmosphere-Ocean, **24**, 201-234.

Wood, L.J., Ethridge, F.G. and **Schumm, S.A.**, The effects of base-level fluctuations on coastal plain-shelf-slope depositional systems: an experimental approach. In: Sequence Stratigraphy and Facies Associations (H.W. Posamentier, C.P. Summerhayes, B.U. Haq and G.P. Allen), Int. Assoc. Sedimentol. Spec. Publ., **18**, 43-54.

Woolfe, K.J., Larcombe, P., Naish, T. and **Purdon, R.G.** (1998) Lowstand rivers need not incise the shelf: an example from the Great Barrier Reef, Australia, with implications for sequence stratigraphic models. Geology, **26**, 75-78.

Wright, V.P. and **Marriott, S.B.** (1993) The sequence stratigraphy of fluvial depositional systems: the role of floodplain sediment storage. Sed. Geol., **86**, 203-210.

Xu Jie, Snedden, J. W., Galloway, W. E., Milliken, K. T. and **Blum, M. D.** (2017) Channel-belt scaling relationship and application to early Miocene source-to-sink systems in the Gulf of Mexico basin. Geosphere, **13**, 179-200.

Yokoyama, Y., Lambeck, K., De Deckker, P., Johnston, P. and **Fifield, L.K.** (2000) Timing of the Last Glacial Maximum from observed sea-level minima. Nature, **406**, 713–716.

Zaitlin, B.A., Dalrymple, R.W. and **Boyd, R.** (1994) The stratigraphic organization of incised-valley systems associated with relative sea-level change. In: Incised-Valley Systems: Origin and Sedimentary Sequences (Eds R.W. Dalrymple, R. Boyd and B.A. Zaitlin), SEPM Spec. Publ., **51**, 45–60.

Zhang Guijia and **Li Congxian** (1996) The fills and stratigraphic sequences in the Qiantangjiang incised paleovalley, China. J. Sed. Res., **66**, 406-414.

Zhang Xia, Dalrymple, R. W. and **Lin Chunming** (2017) Facies and stratigraphic architecture of the late Pleistocene to early Holocene tide-dominated paleo-Changjiang (Yangtze River) delta. Geol. Soc. Am. Bull., **130**, 455-483.

Zhuo Haiteng, Wang, Yingmin, Shi Hesheng, He Min, Chen Weitao, Li Hua, Wang Ying and **Yan Weiyao** (2015) Contrasting fluvial styles across the mid-Pleistocene climate transition in the northern shelf of the South China Sea: Evidence from 3D seismic data. Quatern. Sci. Rev., **129**, 128-146.